Materials Today Bio 14 (2022) 100263

Contents lists available at ScienceDirect

Materials Today Bio

journal homepage: www.journals.elsevier.com/materials-today-bio

Plasmonic nanosensors for point-of-care biomarker detection

Congran Jin [1], Ziqian Wu [1], John H. Molinski [1], Junhu Zhou, Yundong Ren, John X.J. Zhang [*]

Thayer School of Engineering, Dartmouth College, NH, USA

ARTICLE INFO

Keywords:
Plasmonic
Biosensor
Point-of-care
Biomarker
Covid-19

ABSTRACT

Advancement of materials along with their fascinating properties play increasingly important role in facilitating the rapid progress in medicine. An excellent example is the recent development of biosensors based on nanomaterials that induce surface plasmon effect for screening biomarkers of various diseases ranging from cancer to Covid-19. The recent global pandemic re-confirmed the trend of real-time diagnosis in public health to be in point-of-care (POC) settings that can screen interested biomarkers at home, or literally anywhere else, at any time. Plasmonic biosensors, thanks to its versatile designs and extraordinary sensitivities, can be scaled into small and portable devices for POC diagnostic tools. In the meantime, efforts are being made to speed up, simplify and lower the cost of the signal readout process including converting the conventional heavy laboratory instruments into lightweight handheld devices. This article reviews the recent progress on the design of plasmonic nanomaterial-based biosensors for biomarker detection with a perspective of POC applications. After briefly introducing the plasmonic detection working mechanisms and devices, the selected highlights in the field focusing on the technology's design including nanomaterials development, structure assembly, and target applications are presented and analyzed. In parallel, discussions on the sensor's current or potential applicability in POC diagnosis are provided. Finally, challenges and opportunities in plasmonic biosensor for biomarker detection, such as the current Covid-19 pandemic and its testing using plasmonic biosensor and incorporation of machine learning algorithms are discussed.

1. Introduction

The rational design of plasmonic materials has the potential for profound implications within the field of biosensing, drastically increasing sensitivity and lowering limit of detection of assays that incorporate them. The materials and configurations through which this effect is employed has been rapidly expanding, leading to novel particle or structure geometries and/or configurations leading to greater levels of field enhancement. Plasmonic enhancement has been demonstrated to be a largely multifaceted parameter shown to be dependent upon numerous parameters of the overall system, including particle or structure size, geometry, arrangement. morphology, material, areal density, among others [1,2]. As such, there is significant interest in the optimization of these various parameters thereby allowing the rational design of the plasmonic nanomaterials with superior performance.

Of plasmonic nanomaterials, classifications can be developed that differentiate the two main systems reported in literature, namely particle-based systems and surface-based systems. The former class encapsulates efforts of engineering plasmonic nanoparticles based on material, geometry, morphology, size, and functional coatings [3–9]. Particles within these systems are typically fabricated using chemical synthesis methods, which provides significant levels of tunability and repeatability throughout batches. In these systems, the particles are often suspended and stabilized within solutions where the assays are completed. The latter class of surface-based systems consists of nanoparticles or structures upon a surface which can be tuned based on material, size, areal density, geometry, and periodicity [10]. Though this class may include singular particles aggregated upon the surface [2,11], the mechanism and unique optical properties generated by this configuration merits differentiation from the former class. Fabrication methods can vary widely for such systems and prior reports have utilized simplistic processes such as chemical synthesis to advanced lithographic processes.

Currently within the field, there exists an emphasis on exploring various fabrication methodologies and techniques with the focus on the development of tunable plasmonic structures and systems. Though

* Corresponding author.
E-mail address: John.Zhang@Dartmouth.edu (J.X.J. Zhang).
[1] denotes equal contribution.

https://doi.org/10.1016/j.mtbio.2022.100263
Received 26 January 2022; Received in revised form 12 April 2022; Accepted 13 April 2022
Available online 16 April 2022

promising results have been shown with various system configurations, keeping scalability at the forefront of system development will enable future systems to be applicable in point-of-care (POC) settings [12–14]. This application space requires a unique set of attributes not shared with use within clinical setting such as low-cost, scalable, and stable systems. By association, this provides unique challenges concerning fabrication methods employed or system configurations. There are numerous unique considerations that must be considered concerning the design and implementation of plasmonic nanomaterials for POC biosensing applications. Namely, sensor type and structure (i.e., nanoparticle solution or substrate-based), reagent usage and sensor stability, as well as read-out method (i.e., colorimetric, fluorometric, etc.). Each of these factors have been explored in depth in literatures.

Demand for accessible, effective, and affordable management of infectious diseases in resource-limited settings is seeking for rapid, simple-to-use, inexpensive diagnostics for POC testing. Diagnostic criteria for POC testing in these settings are identified by the World Health Organization (WHO) to be 'ASSURED' - affordable, sensitive, specific, user-friendly, rapid, equipment free and delivered to the end-users [15]. Traditional diagnostic methods such as polymerase chain reaction (PCR) and enzyme linked immunosorbent assays (ELISA), although provide reliable diagnosis and post-treatment monitoring, they can hardly be applied in POC situations because they require a mass of manual preparation steps operated by well-trained technicians [16,17]. As well-known POC solution, the lateral flow assays succeed in providing rapid, inexpensive, and semi-quantitative platforms for the detection of detection of various analytes but are held back by inadequate sensitivity and selectivity – especially the cross-reactivity problem [18]. Recently, plasmonic-based biosensors have emerged as a potential solution for disease diagnostics and treatment monitoring at POC [19–21]. They not only enhance the performance of existing platforms, but also provide new-emerging highly sensitive and label-free detection of biomarkers. Fig. 1 provides an overview of typical biomarkers explored within POC diagnostic technologies and those covered within this review. Disease types can vary greatly however biomarker type traditionally falls within four main classes, nuclei acid, antigen/antibody, virus, and bacteria. Nanomaterial based sensor design normally include nanoparticles based designs, on-chip designs and patterned surfaces.

When light impinges from a dielectric medium onto a metallic surface, the electromagnetic (EM) field of the light excites the free electron of the metal to oscillate coherently and forms what is known as the surface plasmon [22]. Mainly two types of surface plasmons have been studied, namely the surface plasmon polariton and the localized surface plasmon (LSP) as shown in Fig. 1. A surface plasmon polariton is an EM surface wave that propagates along the planar dielectric-metal surface (Fig. 2A). A LSP is present when a surface plasmon is confined in a nanoparticle of size close or smaller than the wavelength of the excited light (Fig. 2B). For both the surface plasmon polariton and the localized surface plasmon, there exists a wavelength-specific resonant condition called the surface plasmon resonance (SPR), under which the surface plasmon is most efficiently excited. At the resonance wavelength, enhanced near-field amplitude is present. For localized surface plasmon, the highly localized field at the nanoparticle diminishes dramatically as it distances from the nanoparticle. The resonant interaction between the EM field and the surface plasmon at the SPR condition enables light to efficiently couple the plasmonic metal nanostructures. Such light coupling breaks the diffraction limit and creates an enhanced light-matter interaction at the subwavelength scale. A plasmonic metal nanostructure can have one or several SPR modes, each mode corresponds to a specific SPR wavelength. The SPR wavelength depends on the shape and material of the plasmonic nanostructure. It can also be tuned by nearby polarizable materials and optical cavities and is highly sensitive to the environmental refractive index changes.

The SPR enhanced light-matter interaction has benefited a wide range of biosensing applications. These applications are mainly of two categories. First, biosensors that interrogate the environmental changes through the change of the SPR signal, such as the SPR wavelength shift and SPR intensity changes. Second, biosensors based on a sensing mechanism that is not SPR itself but whose sensor responses are enhanced and augmented by the SPR, such as the SPR enhanced fluorescent imaging and the surface enhanced Raman spectroscopy (SERS) [23,24].

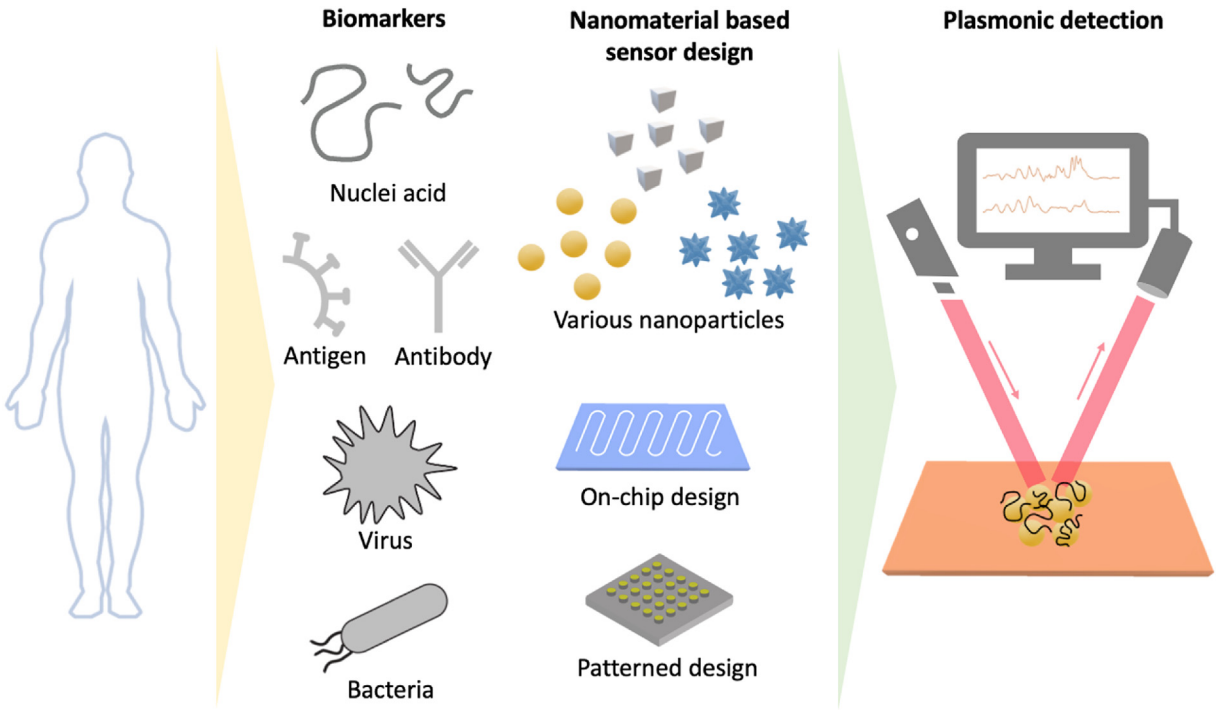

Fig. 1. Overview schematic showing typical biomarkers, the various shapes based sensor designs and plasmonic detection that are explored within point-of-care diagnostic technologies reviewed in this work.

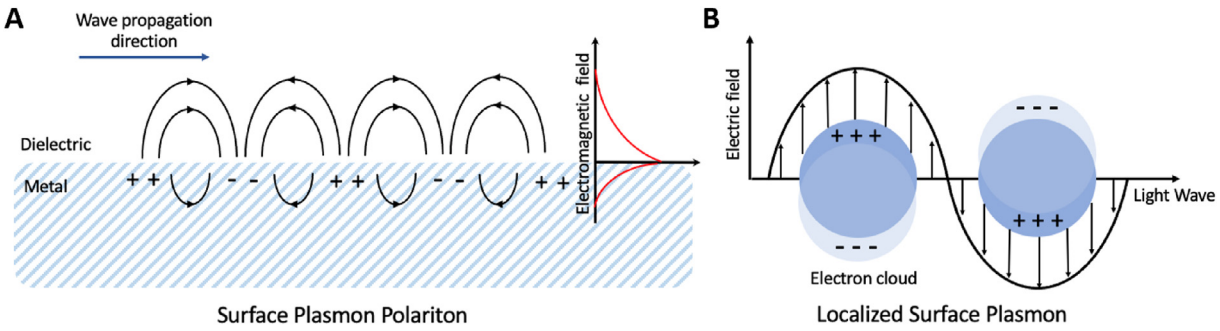

Fig. 2. The schematics of the mechanism of **A.** a surface plasmon polariton and **B.** a localized surface plasmon.

The objective of this work is to provide a comprehensive review of the most recent progress on the design and assembly of plasmonic nanomaterials for POC biomarker detection. We will focus on, firstly, the design and assembly of the nanomaterials and, secondly, the large range of biomarker sensors particularly suitable for POC disease diagnosis. The rest of this work is arranged in the following order. In section 2, optical signal read-out mechanisms will be reviewed, including colorimetric, Raman, fluorescence mechanisms and their corresponding instrumentations. The accessibility and size of these instrument are directly related to whether these techniques are suitable for POC applications or not. Section 3-5 categorize all plasmonic devices into three major groups in terms of their sensing platform structures. Section 3 focuses on reviewing nanoparticles that are used for fabrication of the biosensing platforms. Four different forms of nanoparticles including spheres, cubes, and spikes/stars will be presented. These nanoparticles are either placed in suspension and or on a chip. Different nanoparticles shapes and chip platforms will be categorized and discussed. Next, Section 4 reviews sandwich-, microfluidic-, chip-, and paper-based biosensors with plasmonic mechanism. Microfluidic system is an emerging tool to precisely control nanoparticles geometry and size by confining the chemical reaction in micro channels [24–26]. Paper-based devices are lightweight, small, easily portable, and are therefore extremely suitable for POC diagnosis. Section 5 reviews biomarker sensors with carefully patterned meta-surface using different techniques such as sputtering, photolithography and chemical growth. Section 6 provides the author's perspectives on the challenges and opportunities in the field of plasmonic biosensors for biomarker detection. The example of using plasmonic biosensor for detecting SARS coronavirus-2 virus is discussed. Lastly, this paper is concluded by a summary of the works reviewed.

2. Signal read-out method

Due to the various manifestations of the plasmonic effect and inherent properties of materials demonstrating this effect, there exists numerous potential means to read out a signal from plasmonic nanomaterials. This section will cover main methods exploited including colorimetric, Raman, fluorescence, and handheld device assisted methods (Fig. 3).

2.1. Colorimetric

Colorimetric plasmonic sensing of target analytes has been a largely sought-after approach due to the simplistic nature and lack of dependency on complex instrumentation. Fundamentally, this process relies on the localized surface plasmon resonance (LSPR) of the underlying particle which, because of changes in the local refractive index, will shift the particles resonance wavelength. This shift is typically detected spectroscopically, and the position depends on several factors that will be discussed later in detail. For use within sensing, particles are often conjugated to target a specific analyte of interest, and the new complex is detected by shifting of this resonance wavelength, indicating presence, and by magnitude, concentration of the analyte of interest. Due to the

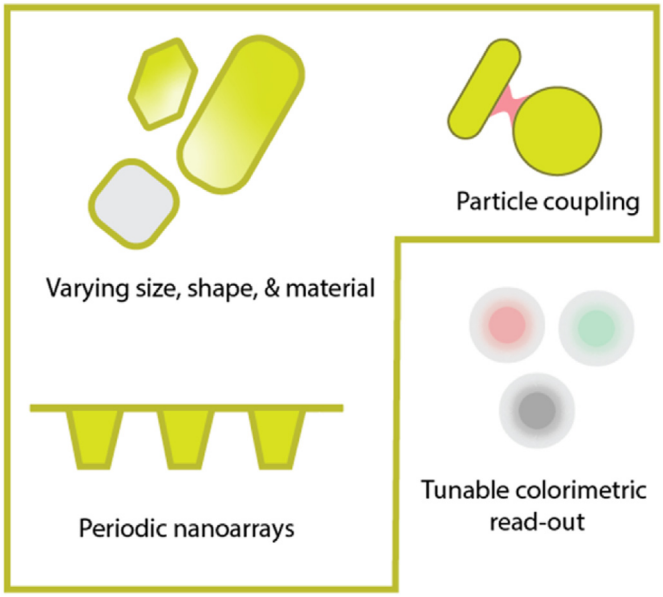

Fig. 3. Overview figure showing the various techniques used for colorimetric detection using plasmonic structures, namely, varying shape, size and material, particle coupling, and periodic nanoarrays.

ability to control a number of parameters surrounding the particles within the system, including material, shape, size, interparticle distance, and composition, there exists significant potential for tunability leading to varying levels of sensitivity. However, for specific materials and configurations it exists within the visible regime and in practice this shift within the visible regime can manifest into a characteristic color change, detectable using only a smartphone camera. In the simplest sensor embodiment, this method utilizes plasmonic nanoparticles within solution or within an array which results in a distinct and characteristic color upon analyte binding. Most commonly, such particles are fabricated through chemical synthesis, and tunability arises from changes in the chemical used or synthesis procedures. Due to the potential for scaling of such methods, there is significant potential for colorimetric read-out methods to be used within POC settings, thus a significant portion of work within this space targets this use-case and applications include medical diagnostics and agriculture.

Due to the amount of work completed within this field, there has been extensive efforts to characterize and optimize a number of different design parameters and their effect on the refractive index sensitivity and visible colors of the particles. Efforts have targeted both computational optimization and experimental investigation and have studied changes in particle shape, material formulation, size, and distance between particles. Shapes including nanospheres, nanorods, nanocubes, nanobipyramids, nanoflowers, nanostars, and nanoplates have been

previously reported [27], whereas those with generally sharper geometries or edges have traditionally been shown to have higher enhancement levels [28,29]. Of recent, particle size has been demonstrated to be a significant factor governing near-field enhancement thus regardless of shape, optimization of size, if possible, is warranted when designing sensors [1]. Traditionally, particles are fabricated using chemical synthesis methods and most commonly are fabricated from gold, due to the LSPR falling within the visible regime. Once synthesized, particles can be functionalized and changes in the near-field such as that due to analyte binding detected using spectroscopy methods. An interesting alternative

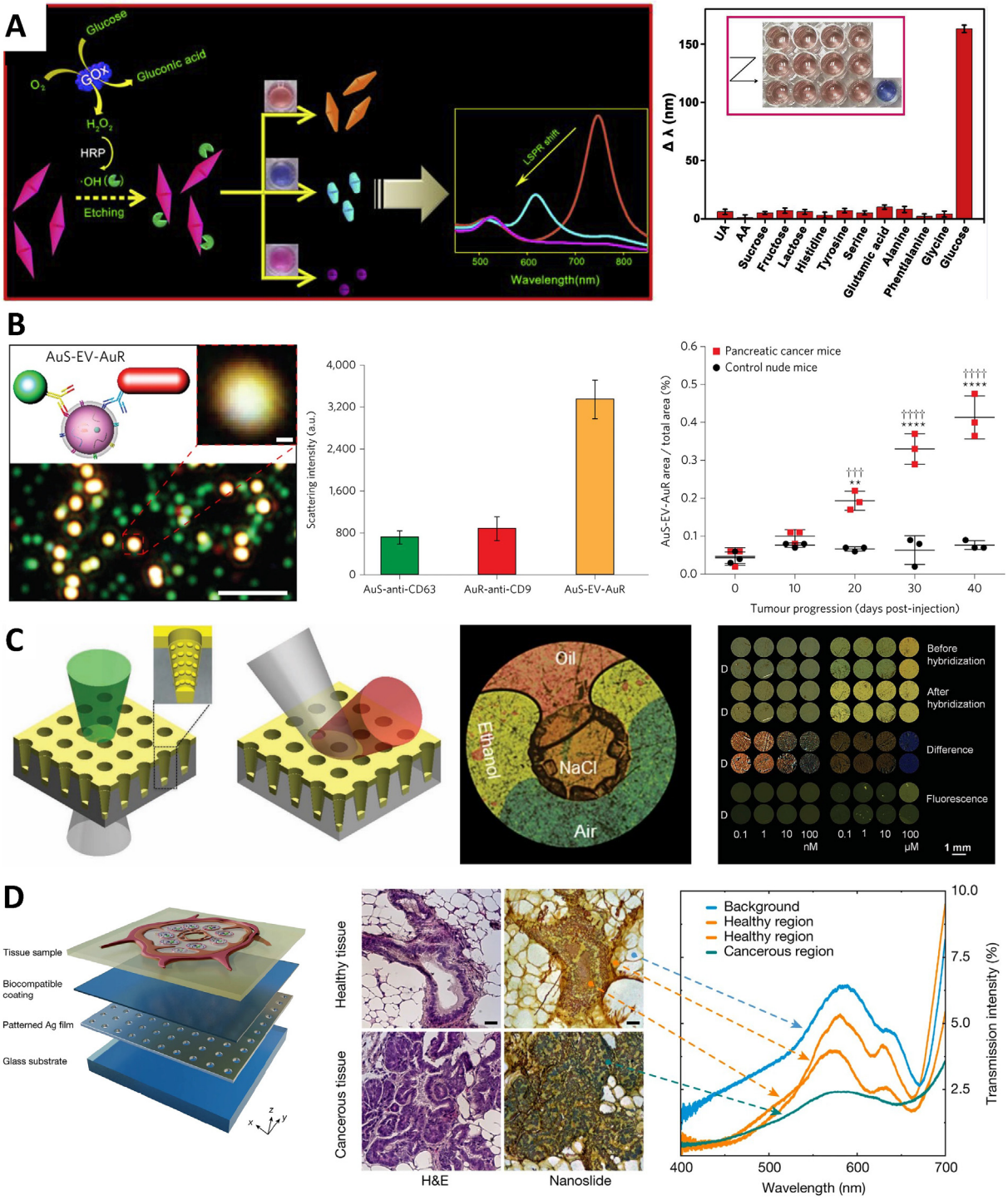

Fig. 4. Colorimetric plasmonic sensing. **A**. A method of colorimetric detection enabled by etching of gold nanobipyramids within an assay, resulting in characteristic solution color changes. This was utilized within for the specific detection of glucose within a patient cohort and enabled the discrimination of healthy and diabetic patients. Replicated with permission from Ref. [31]. **B**. A method for the detection of tumor-derived extracellular via coupling of plasmonic particle which demonstrates enhanced scattering. Replicated with permission from Ref. [33]. **C**. A nano Lycurgus Cup array which demonstrates high refractive index sensitivity (46,000 nm/RIU) and enables colorimetric detection of varying refractive index environments, such as that within DNA solutions of varying concentrations. Replicated with permission from Ref. [10]. **D**. A method for colorimetric histology using patterned silver films, enabling the detection of tissues by subtle changes in the dielectric constant of various tissues. Replicated with permission from Ref. [39].

to this approach which enables the colorimetric detection of analytes is through post-synthesis etching or growth, enabling further tuning of particle morphology and thus properties [30]. In one such study using this approach, colorimetric detection of blood glucose was enabled by changing the morphology of the gold nanobipyramids within an assay through enzymatic etching resulting in a characteristic solution color change detectable by the naked eye [31] (Fig. 4A). Within the assay, glucose oxidase oxidizes glucose forming H_2O_2 which is subsequently broken down into hydroxyl radicals in the presence of horseradish peroxidase which accelerates initial nanobipyramid etching. Using this method, they showed a dynamic range of 0.05–90 μM, limit of detection of 0.02 μM, time to result of 30 min, and good correlation with traditional hospital detection methods. They lastly employed the sensor for glucose sensing within serum of a small cohort of healthy people and diabetic patients and enabled differentiation of the two groups through naked eye detection alone.

Though single particles within solution represent the predominate sensor configuration utilized, there has been intriguing recent advancements which utilize coupled particle systems as a means for detection. Such approaches make use of the plasmonic "hotspot", or the highly enhanced EM field between nearby and interacting plasmonic nanoparticles. This phenomenon has been robustly investigated computationally and experimentally using nanofabricated samples which provides significant control over sample size, shape, spacing, and thus properties [32]. However, for use within POC settings there has been significant interest in finding alternative fabrication methods that are amendable to scaling. In one such study, Liang et al. [33] took advantage of the unique plasmonic properties of two morphologies of chemically synthesized plasmonic nanoparticles, a gold nanorod and gold nanosphere (Fig. 4B, left). Independently, the plasmonic properties of these two distinct particles have been well studied in literature, with robust links between varying size and shape of particles and characteristic resonance wavelengths. In this study, 50 nm AuNSs with a resonance peak of ~550 nm which scatters green light was coupled with 25 × 60 nm nanorods with a resonance peak of ~650 nm which scatters red light. When these two particles were close enough to one another (<200 nm), the particles interact with another, leading to coupling and scattering of yellow light with a significantly higher intensity than either individual particle (Fig. 4B, middle). This was used as the basis for an assay by functionalizing both nanoparticles to bind to protein markers on the surface of extracellular vesicles (30–150 nm in diameter), CD63 and CD9. As a result, the binding of both particles to a singular extracellular vesicle would enable detection using dark-field microscopy. This method provided detection of circulating extracellular vesicles in as little as 1 μL of plasma and enabled differentiation between pancreatic cancer, pancreatitis, and normal controls based on area ratio, a metric that considers the signal area versus background as a proxy for concentration [33] (Fig. 4B, right).

The ability to detect multiple analytes within a single test, multiplexed detection, lowers cost and simplifies the diagnostic workflow significantly. As such, there has been significant interest in combining plasmonic nanoparticles within single assays to allow for the differentiation and detection of multiple analytes simultaneously. The significant levels of tunability within system design and configuration when it comes to particle-based systems makes them an ideal candidate for such assays. A straightforward approach to achieve multiplexing is by changing the shape between multiple underlying particles within the system, however this increases complexity when it comes to chemical synthesis as each particle need to be synthesized independently. A simpler alternative approach which has been investigated is multiplexing spatially, by patterning specific areas within the assay with unique particles or structures. In this manner, theoretically the same particles can be used in multiple areas of the assay, as long as it is spatially accounted for, both reducing assay complexity and increasing repeatability. In a recent study in this field, Pinheiro et al. [34] utilized configurable gold nanoparticles for colorimetric multiplex detection of glucose, uric acid, and free cholesterol in a single paper-based microfluidic assay. This work made use of *in situ* gold nanoparticle synthesis for the detection of glucose and demonstrated detection at physiologically relevant ranges with a limit of detection of 1.25 mM. For the other two analytes, tailored gold nanoparticles were used to functionalize paper and the optical properties altered by changing degree of aggregation. Due to the addition of multiple techniques leading to colorimetric detection, the development and optimization of such an assay is quite involved, however preliminary results are encouraging. Another example to achieve multiple readouts is provided by Wang et al. [35] by utilizing the catalytic-regulated gold nanoparticle etching process. Aggregation behavior, catalytic activity and etching level are used in the system as triple sensing channels for protein discrimination, which can be well reflected by the color change of solution. The differentiation of pure protein and protein mixtures is validated through urine sample.

Plasmonic particle-based systems, mainly those for solution-based sensing, represent a significant portion of the colorimetric sensors reported thus far in literature, however of recent there has been advances that utilize periodic nanoarrays that enable colorimetric sensing. Although fabrication of these systems is more complex, requiring specialized equipment and lengthy processing stages, the ability to pattern these upon surfaces provides unique potential and integrates well with standard clinical sample processing. This field is still early in its development, however if methods are developed that reach scalability of particle-based system then there exists significant potential or POC assay development. Gartia and coworkers [10,36–38] developed a periodic nanolycurgus cup array and demonstrated its potential for colorimetric detection of refractive index environment changes such as in the presence of air, oil, ethanol, and NaCl solution (Fig. 4C). In this study, due to the high sensitivity (~46,000 nm/RIU) they further showed colorimetric sensing directly upon the fabricated surface via changes of DNA concentration within solution [10] (Fig. 4C). Though the fabrication of such a sensor requires specialized equipment and nanofabrication techniques, it provides an intriguing proof-of-concept platform that would be largely applicable in biosensing if scalability was achieved. In another example, Balaur et al. [39] developed a plasmonic microscope slide that allows colorimetric histology of tissues without the use of staining by transducing minute changes in the dielectric constant of various tissue types into visibly detectable color changes (Fig. 4D). In this paper, they showed the feasibility to differentiate between normal epithelium, usual ductal hyperplasia, and early-stage breast cancer within a diagnostic cohort. Such a system in its current embodiment has little to no POC relevance, but it's likely that such a configuration would also allow for robust surface-based colorimetric sensing. Intriguing results have been presented within literature, however, there still exists high dependence on nanofabricated samples and lithographic methods to enable colorimetric sensing. Considering the ideal use-case for this detection method, POC applications, there needs to be further development into similarly sensitive, yet scalable fabrication methods.

2.2. Fluorescence, Raman, and handheld-format systems

Fluorescence is a photoluminescence process where a fluorophore molecule absorbs a photon and then emits a photon of lower energy (longer wavelength). Roughly, the fluorescence process can be separated into three steps. First, the fluorophore molecule absorbs the photon and is put into an excited state. Then, the excited fluorophore molecule converts to a lower energy without emitting any photons. Finally, the excited fluorophore radiatively decays to a lower energy and emits a photon. In these three steps, while the second step is independent of the excitation light intensity, the efficiency of the first and third steps can be enhanced by a higher excitation light intensity.

Raman spectroscopy is a technique used to identify molecules by providing a molecular fingerprint. Its working mechanism relies on inelastic scattering of light, or specifically, photons, which is also called Raman scattering. When an incident light or a group of photons pass the

sample with a photon frequency v_i, some will leave the sample in a path along the direction of the incident light, which is called transmitted light, while others will leave the sample in all other directions, which is called light scattering. For the scattered photons, when their frequency (v_s) equals the frequency of incident light (v_i), or $v_i = v_s$, Raleigh scattering, occurs. When they are not equal, or $v_i \neq v_s$, Stokes scattering occurs. Raleigh scattering is elastic scattering while Stokes scattering is inelastic scattering. There are two energy scenarios when $v_i \neq v_s$. As the incident photon interact with the electron cloud of the sample, the vibrational energy of the electron cloud either gains energy (goes to a higher energy level) or loses it (goes to a lower energy level) after the photo is emitted out (Fig. 5A). Correspondingly, to maintain the total energy in the system, the emitted photon will either have a lower energy (lower frequency) when the electron adsorbs energy or a higher energy (higher frequency) when the electron lose energy. If the emitted photon's energy (or frequency) is smaller than that of incident photon, or $v_s < v_s$, Stokes scattering will be observed. On the other hand, if the emitted photon's energy (or frequency) is larger than that of incident photon, or $v_s > v_s$, Anti-stokes scattering will be observed (Fig. 5B). These shifts in energy, also called Raman shift, provide information about the vibrational mode in the sample molecules. Hence, Raman can be used to reveal the identity of the sample molecule by comparing the observed shifts in frequencies to those known substances. In addition, the intensity of those peaks represents the number of photons received by the detector. The higher the intensity, the more photons are detected. By this means, Raman can quantitatively measure the concentration of the sample.. As shown in Fig. 5C Conventional Raman spectroscopy has a big and bulky machine body that include all the optical components in it such as a microscope, lens, lasers, filters, etc., which can be hardly adapted to POC applications due to their bulky size. However, more recently, handheld Raman spectrometer (Fig. 5D) has emerged in the market that make Raman detection and analysis easily and conveniently accessible, opening a new revenue for its applications in the realm of POC medical diagnostics.

While many portable diagnosis platforms emphasize convenient detection through bare eyes, it is notable that detection error from bare eyes can sometimes lead to significantly inaccurate diagnosis results. Thanks to the rapid development of computing techniques and miniaturized chips, smartphones have become a highly integrated sensing and computing system, thus playing a vital role in the portable diagnosis platform for fast and accurate detection for POC applications.

The sensing capability of smartphones that has been predominantly utilized in the mobile diagnosis platform is their imaging camera. In typical colorimetric assays, a biochemical reaction takes place to introduce a distinguishable color change in the solution or chip to enable detection of analyte. With the use of smartphones, the color transition or color intensity is captured through the cameras and followed with image processing techniques and a variety of computations to quantify the concentration of detected analyte. Examples of smartphone readers for colorimetric sensing includes the detection of ascorbic acid in tear fluid by Misra et al. [40], detection of human C-reactive protein with graphene-based microliter plate in diluted human whole blood by Vashist et al. [41], detection of cancer antigen 125 (CA125) through functionalized Au–Ag NPs by Hosu et al. [42], and detection of bacteria by Zheng et al. [43] In other studies, researchers develop smartphone-based imaging platforms to serve as a household instrument for plasmonic detection and analysis software. For instance, Lee et al. [44] combined a highly sensitive SPR biochip and a simple portable imaging setup for label-free detection of imidacloprid pesticides. Their plasmonic chip showed spot shift in response to changes of pesticide concentration, which can be accurately detected through imaging of smartphone and do quantitative analysis. Another hand-held SPR imaging platform was developed by Guner et al. [45] which is composed of SPR sensor chips and a smartphone-based compact optical system (Fig. 6A). The silver/gold (Ag/Au) bilayer structure coated Blu-ray disc sensor chips were capable to perform plasmon resonance imaging at the central region of visible spectrum, and the image intensity was captured through the smartphone to estimate the analyte concentration. Smartphone is also reported to be applied for fluorescence imaging by Lee et al. [46], as shown in Fig. 6B. In this study, Lee et al. performed a smartphone-based fluorescence microscopy to do dual-wavelength fluorescent detection of 17-β-estradiol in water. The smartphone's camera is connected to a microscope with a band-pass filter to display the two channels fluorescent images of the sensing array with high resolution. More recently, Bian et al. [47] proposed a metasurface-inspired

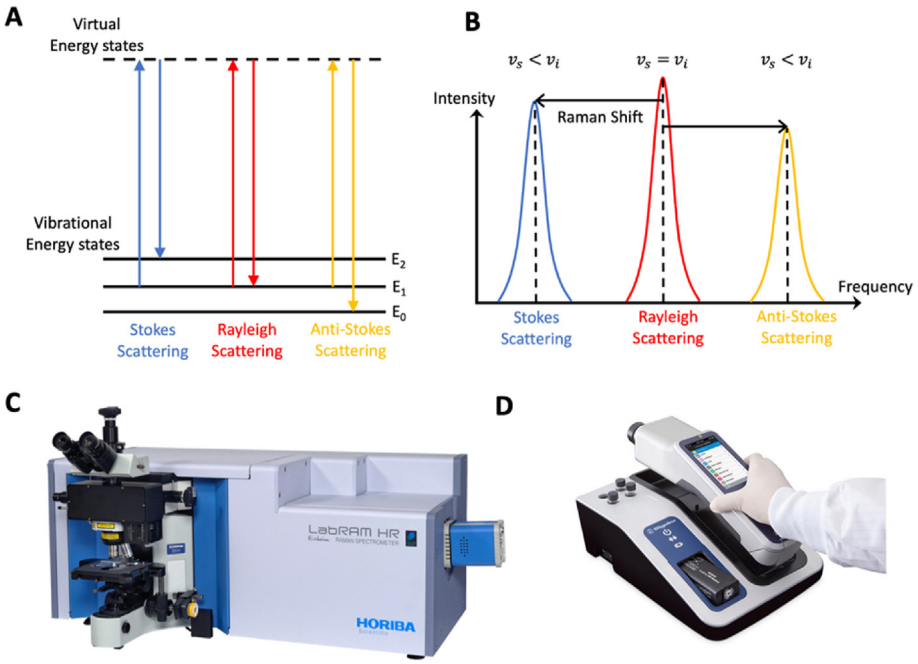

Fig. 5. Raman Spectroscopy. **A.** The change of vibrational energy states in the process of a photon interacting with sample molecule. **B.** A Raman spectrum showing three different energy shift scenarios. **C.** A Raman spectroscopy machine. Photo credit by Horiba, Ltd. **D.** A handheld Raman spectrometer. Photo courtesy of Rigaku Analytical Devices.

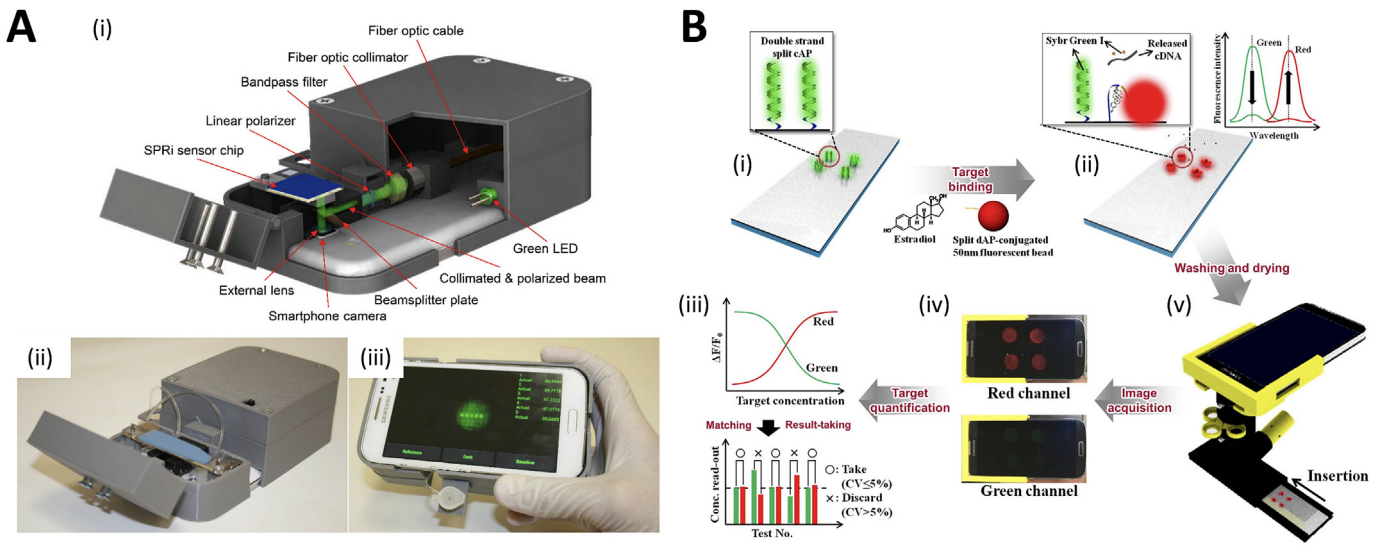

Fig. 6. Hand-held Devices and systems. **A**. SPR imaging platform integrated with a smartphone. Replicated with permission from Ref. [45]. **B**. A schematic illustration of the overall work design for the dual wavelength fluorescent detection. Replicated with permission from Ref. [46].

Table 1
Summary of representative nanoparticle based plasmonic biosensors developed recently.

Particle form	Synthesis method	System/Method	Disease detected	Biomarker	POC ability	Limit of detection	Ref.
Spheres	Hydroxylamine hydrochloride reduction (Ag)	SERS	HBV	L-arginine, nucleic acid	Low	N/A	[48]
	Citrate Reduction (Au)	Colorimetric sensing	HBV	Hepatitis B surface antigen (HBsAg)	High	1 pg/mL	[49]
	Seed-mediated growth (Au)	Colorimetric sensing	HIV	HIV template DNA	High	0.01 zmol	[50]
	Citrate reduction (Au)	SERS	HIV	HIV-1 DNA	High	0.24 pg/mL	[51]
	Citrate reduction (Au)	Colorimetric sensing	TB	TB DNA	High	19.5 pg/mL	[52]
	Commercial product (Au)	SERS	TB	ManLAM	Low	NA	[53]
	Commercial product (Au)	Toroidal electrodynamics	COVID-19	SARS-CoV-2 spike protein	Medium	4.2 fmol	[54]
	Citrate Reduction (Au)	colorimetric sensing	epithelial ovarian cancer	cancer antigen 125	High	30 U/mL	[55]
	Citrate reduction (Au)	Colorimetric sensing	COVID-19	SARS-CoV-2 RNA	High	0.18 ng/μL	[56]
Cube	Seed-mediated growth (Au)	LSPR	Lung cancer	MiR-205	Medium	5 pM	[57]
	Chemical reduction (Au) Seed-mediated growth (Ag)	LSPR	Hypo/hyperkalemia	Potassium	Low	1 nM	[58]
	Seed-mediated growth (Ag)	SERS	Mycotoxin	Ochratoxin A	Medium	0.01 nM	[59]
	Sulfide-mediated method (Ag)	SPR	n/a	Immunoglobulin G (igG)	Medium	0.6 μg/mL	[60]
	Chemical reduction (Ag)	SERS	Toxicity	Dithiocarbamate (DTC)	Low	44 nM	[61]
Spike/star	Seed-mediated growth (Au)	SPR	n/a	Genomic DNA	Medium	6.9 fM	[62]
	One-pot seedless protocol	SERS	Hand, food and mouth disease	Enterovirus 71	High	107 pfu/mL	[63]
	Ascorbic acid reduction (Au)	SPR	Influenza A	H5N1, H4N6	Low	0.0268 HAU/50 μL	[64]
	Chemical reduction (Au)	SERS	Mosquito-borne diseases	Nonstructural protein	Medium	55.3 ng/mL	[65]
	Chemical reduction (Au)	SERS	Oxidative stress and related diseases	Hypochlorite (ClO−) and glutathione (GSH)	Medium	0.40 μM	[66]
	Sputtering (Au)	SERS	Influenza	Influenza antibody	Medium	10 pM	[67]
Other nanostructures	Seed-mediated Growth (Au)	LSPR	TB	CFP-10 ESAT6 antibody	High	N/A	[68]
	Seed-mediated Growth (Au)	LSPR	Tumor	ctDNA	Medium	2 ng/mL	[69]
	NIL and thin-film (Au)	Plasmonic fluorescence	Ebola	EBOV antigens	Medium	220 fg/mL	[70]
	Simulation	SPR	COVID-19	SARS-CoV-2 spike protein	Low	111.11 deg/RIU	[71]
	Commercial product (Au)	LSPR	HIV	HIV-1 p24 antigen	Low	10^{-5} pg/mL	[72]
	seed-mediated growth (Au)	LSPR	HBV	Hepatitis B surface antigen (HBsAg)	Medium	100 fg/mL	[73]
	Electrodeposition (Au)	LSPR	COVID-19	SARS-CoV-2 spike protein	High	0.08 ng/mL	[74]
	Boiling reduction (Au) on magnetic NP	SPR	TB	anti-CFP-10	Low	0.1 ng/mL	[75]
	DNA template (Ag/Pt)	Colorimetric	Cancer	miRNA-21	High	0.6 pM	[76]
	Dipping (Au)	Plasmonic fluorescence	Malaria	PfLDH	Low	1 pg/mL	[77]

biosensor, patterned plasmonic gradient, together with a smartphone for high precision sensing. The patterned plasmonic gradient transduced local index information into 2D patterns by forming visible resonance contour lines for easy readout. The smartphone was connected to a microscope to directly read the 2D patterns with high sensitivity and do the real-time analysis with a homemade program.

3. Nanoparticle based designs

Most plasmonic biosensor utilize plasmonic nanoparticles to induce or enhance surface plasmon effect. In designing these nanoparticles-based sensors, different particle forms, shapes, fabrication methods and working mechanisms are employed to produce devices that detect different biomarkers and diseases such as hepatitis B virus (HBV), human immunodeficiency virus (HIV) and tuberculosis (TB) with various limit of detection. Table 1 summarizes these characteristics of some the most representative devices developed recently that are based on nanoparticles. In addition, the potential of these devices' POC applicability is evaluated. In the following sub-sections, we categorize the plasmonic nanoparticles into three major forms including sphere, cubic, and spike/star structures and reviewed and discussed their role in biosensors.

3.1. Sphere

As early as the late 19th century, the topic of interaction between light and small particles, especially colloidal particles of gold and silver, has been attractive to researchers [78,79]. It is widely known that the EM field around the surfaces of the nanoparticles exhibits strong resonant and oscillating behavior – which is called plasmon resonance if light with appropriate wavelength is incident. Various nanostructures have been fabricated, characterized, and applied in applications through decades of development on nanomaterial fabrication techniques, such as self-assembly, chemical growth and lithography. However, nanospheres are still primarily used in plasmonic sensors due to their easy fabrication process and low-cost. In addition, significant enhancement of light occurs in the narrow gap regions when plasmonic nanospheres are closely coupling [80].

Chemical growth is the most popular method to synthesize Au and Ag nanospheres of different sizes. Turkevich et al. first developed the single-phase-based reduction of gold or silver salt by citrate to fabricate size tunable nanospheres [81]. 40 years later, Brust introduced a two-phase (water-toluene) reduction of $AuCl_4^-$ to prepare 1–3 nm gold nanospheres (AuNSs) bearing a surface coating of thiol [82]. For the synthesis of plasmonic AuNSs, gold chloride trihydrate ($HAuCl_4$) is the most commonly used precursor, which requires reducing agent such as trisodium citrate or sodium citrate to initiate the reaction [83–86]. Seeding-mediated fabrication based on the separation of nucleation and growth is also used to synthesize citrate-stabilized AuNSs with the diameter up to ~200 nm [87,88]. Silver nanospheres (AgNSs) can be fabricated in a similar way. For example, by reduction of silver nitrate ($AgNO_3$) with hydroxylamine hydrochloride at alkaline pH, highly SERS-active AgNSs with diameters between 23 and 67 nm are produced [89,90].

Pure nanospheres without further functionalization can be feasible for label-free disease detection. For instance, Yudong et al., directly mixed blood serum from patients confirmed with HBV and healthy volunteers with AgNSs solution at 1:1 ratio for SERS measurement [90]. By comparing Raman bands and first order derivative SERS data in the serum SERS spectrum between HBV patients and healthy volunteers, especially the peak position of biomolecules (like L-arginine and saccharide) that were relevant to HBV transformation and infection, they achieved a non-invasive and accurate diagnostic of HBV detection in 10 minutes. Another way to utilize pure plasmonic nanospheres for biosensing is through seed-mediated growth. The mechanism is to take advantage of reducing agent produced in physiological processes or reactions in the sample, such as NADH, to reduce $HAuCl_4$, which results in the enlargement of AuNSs. The color change caused by the enlarged AuNSs is a convenient and robust signal for colorimetric assay. For example, Peng et al. developed a colorimetric sensing method based on alcohol dehydrogenase catalyzed AuNSs growth for the detection of the hepatitis B surface antigen (HBsAg) [91]. In the plasmonic ELISA design, they attached streptavidin-alcohol dehydrogenase (ADH) to biotinylated secondary antibodies, so that biocatalytic cycle can be catalyzed between NAD^+ and ethanol to generate NADH (Fig. 7A). Therefore, in the presence of antigen (HBsAg), the size of AuNSs enlarged and the solution color changed from yellow to purple. Comparing to other sophisticated methods, it provides POC ability to detect any disease biomarkers as long as appropriate antibodies exist.

Functionalized nanospheres provide even more possibilities in biomarker detection. Since Mirkin modified AgNSs with polynucleotides to achieve colorimetric detection based on the concentration of target molecule [92], enormous effects have been made for the development of nanospheres surface functionalization with different probes to provide highly sensitive and specific detection of a wide range of markers. Detection of DNA, RNA and oligonucleotide has received the greatest attention. Capping rationally designed thiol-modified antisense oligonucleotides onto AuNSs is a simple and straightforward approach for diagnosing. For example, Moitra et al., developed a colorimetric assay based on oligonucleotides capped AuNSs specific for N-gene of SARS-CoV-2, which diagnosed positive COVID-19 cases within 10 minutes [86]. Such modified AuNSs bunch up only in the presence of target RNA sequence, and lead to a change in SPR with a redshift of ~40 nm in absorbance spectra (Fig. 7B). More importantly, the colorimetric detection can even be recognized by naked eye without complicated instrument, which complies with the ASSURED criteria for POC testing. Tsai et al., shows that when ssDNA modified AuNSs is combined with target dsDNA, the DNA hybridization affects the zeta potential of the AuNSs, resulting in aggregation of the colloid and thus a colorimetric change [85], as shown in Fig. 7C. They extends the sensor to a paper-based system so that the colorimetric results can be rapidly analyzed by smartphone instead of sophisticated equipment. In addition to nucleic acids, antibody or antigen are frequently used in nanospheres surface modification since they have similar complementary counter parts. For instance, Ahmadivand et al., conjugated AuNSs with the monoclonal antibody targeting at spike protein (S1) of SARS-CoV-2 virus and measured the toroidal dipole-resonant shift with different spike protein concentrations (Fig. 7D) [93]. The authors demonstrated that dispersing antibody capped AuNSs to toroidal metasurfaces promoted the binding strength of biomolecules, and they achieved a limit of detection down to ~4.2 fM. Recently, an entropy-driven DNA amplification networks have been achieved using photostable Au–Ag hollow porous nanospheres [94]. Rather than amplify the DNA hairpins, this platform increases double-stranded assembly structures. Au–Ag nanospheres are engineered to be hollow and porous for excellent photothermal conversion efficiency. Apart from nucleic acids, functionalized Au nanospheres also show promising applications in various protein detection. For instance, Jiang et al., [95] developed a sensor platform consisting of AuNPs complexed with aptamers to detect exosomal proteins. The exosomes bind to the aptamers, resulting in the aggregation of AuNPs and a visible color change that can be detect by naked eyes.

Although broadly used as plasmonic materials, metal nanoparticles alone are limited by their low tunability and short lifetime. Surface plasmon hybridization of metal nanoparticles and other nanostructures can enhance the plasmonic properties and provide better sensing performance. For example, Rostami et al., [96] developed a sensing platform by integrating graphene nanoribbons and sliver nanoparticles. The presented hybrid sensor is capable of detecting dopamine and glutathione in sequence by showing a color change from green to red (dopamine) and to grey (glutathione) in human serum samples. DA and GSH were successfully detected in low concentrations of 0.04 μM and 0.23 μM, respectively.

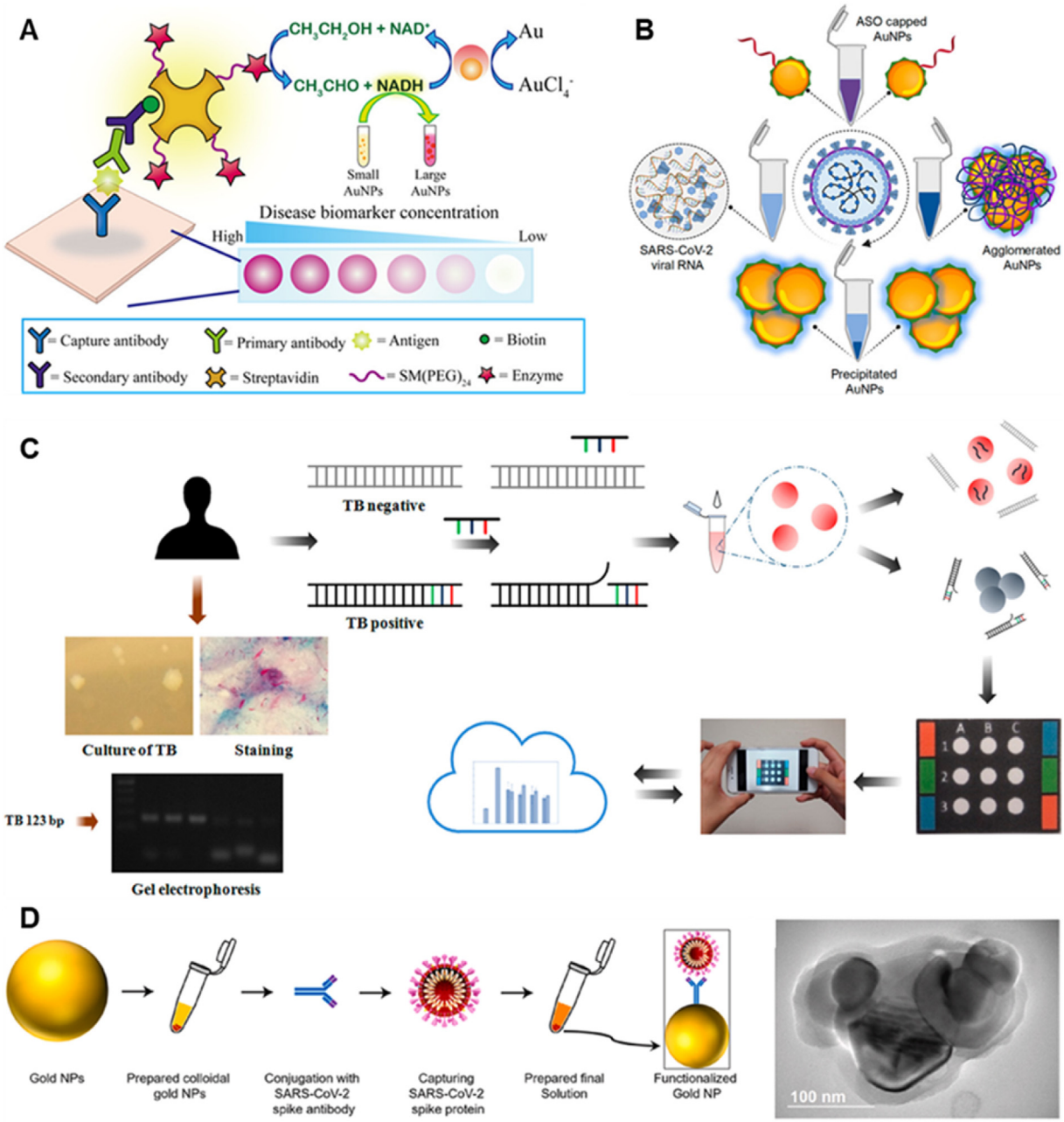

Fig. 7. Nanospheres-enabled biosensors for diseases detection. **A**. The schematic diagram of plasmonic ELISA using AuNSs seed-mediated growth principle. Replicated with permission from Ref. [91]. **B**. The schematic representation for the detection of SARS-cov-2 RNA mediated by the antisense oligonucleotides (ASOs)-capped AuNSs. Replicated with permission from Ref. [86]. **C**. The schematic illustration of the tuberculosis diagnostic method. Replicated with permission from Ref. [85]. **D**. The schematic for the workflow of the SARS-cov-2 spike proteins-AuNSs conjugate and TEM image of conjugated structure. Replicated with permission from Ref. [93].

3.2. Cube

Nanocubes have also drawn great attention in plasmonic sensing for their numerous advantages. Nanocubes have large and uniform faces that can be readily attached to peptidoglycan layer and stay that way, offering antibacterial effect via enzyme-like activities [97]. Jeon and co-workers [98] fabricated and compared Au nanospheres and nanocubes with vertices. The shape effect on the refractive index sensitivity is compared for their LSPR performance. They found that single Au nanocubes with vertices are more sensitive in refractive index than single Au nanospheres of similar size. Nanocubes also provide high electrocatalytic activities than their spherical catalysts counterparts as result of their abundant (100) faces [99,100]. For instance, Au coated Pd nanocubes were placed on networks of single-walled carbon nanotubes (SWCNTs) for building a highly sensitive electrochemical biosensing platform [101]. Platinum (Pt) nanocubes were used to build an amperometric glucose biosensor to increase the activity of the oxidation and reduction of H_2O_2 [102]. In another work, a non-enzymatic glucose sensor was developed by Yang et al. [103] using electrospun Au nanocubes decorated on vertically aligned multi-walled carbon nanotube (MWCNTs) arrays. Further, many research indicate that polyhedral nanoparticles such as nanocubes which have many edges and vertices tend to have stronger localized surfaces plasmon resonance than rounder particles such as nanospheres [58,104,105].

Au and Ag are the two most commonly used materials for fabricating nanocubes for plasmon enhancement. Dr. Xia is one of pioneers of synthesizing high quality, uniform Ag nanocubes [106–108], and many later works that use Ag nanocubes for plasmon biosensing either directly

employed his protocol or with slight modification. In Xia's method [106], Ag nanocubes are fabricated using polyol synthesis method where ethylene glycol is used as the reducing agent and the solvent. Na_2S is then added to the system. Ag_2S nanocrystallites, which can reduce $AgNO_3$, are generated after $AgNO_3$ is added to the solution. This rapid reduction process helps shape the formation of Ag cube. Poly (vinyl pyrrolidone) (PVP), which selectively binds to Ag's {100} facets, also contribute to the formation of Ag cubes. For the fabrication of Au nanocubes, a two-step seed-mediated growth method is usually employed [109]. In the first step, the Au seed is prepared by quick addition and mixing of ice-cold $NaBH_4$ solution into a mixture solution of $HAuCl_4$ and cetrimonium bromide (CTAB). In the second step, the growth solution is made by mixing water, $HAuCl_4$, CTAB and ascorbic acid which the seeds solution is added to. The mixture solution stays at room temperature overnight followed by wash and centrifugation process to obtain the Au nanocubes.

Before researchers utilized the plasmonic effect to enhance the signal of silver nanocubes for biosensors, they simply use Ag nanocubes for its electrochemical properties such as the electron transfer effect with H_2O_2 . For example, Yang et al. [100] designed an amperometric bienzyme biosensor for glucose detection using Ag nanocubes and Au electrode. The substrate for the Ag nanocubes is horseradish peroxidase (HRP)-chitosan (CS)-glucose oxidase (GOx) bienzymatic film. The working mechanism for this biosensor involves reduction of H_2O_2 which is produced in the enzyme reaction. The chemical reaction can be expressed with equations (1)–(3) [100]. Similarly, Yang et al. [103] built a non-enzymatic glucose sensor based on Cu nanocubes electrodeposited on vertically aligned multi-walled carbon nanotubes (MWCNTs). It is demonstrated that this sensor showed enhanced electrocatalytic activity to glucose oxidation in NaOH solution. Ren et al. [102] promote the electrocatalytic activity of the oxidation and reduction of H_2O_2 by fabricating an amperometric glucose biosensor. In this design, Pt nanocubes are used to facilitate the electron transfer activity which significantly increase by H_2O_2 which is produced in the glucose oxidization process by GOx.

$$Glucose + O_2 \rightarrow Gluconic\ acid + H_2O_2 \quad (1)$$

$$H_2O_2 + 2H^+ + Ag \rightarrow 2H_2O_2 + Ag^+ \quad (2)$$

$$Ag^+ + e^- \rightarrow Ag \quad (3)$$

Zhang et al. [57] designed a cancer biomarker detector based on plasmonic effect using Au nanocubes. The mechanism of the sensor is based on the increase in reflective index induced by hybridization on the surface of Au nanocubes which are modified by thiolated single strand DNA (ssDNA) (Fig. 8A). The device's sensing capability is demonstrated by detecting microRNA205 (miR-205) which is an important tumor biomarker. It is shown in the experiment that the limit of detection reaches as low as 5 pM in serum samples. A recent work also reported that Au nanocubes with flat surfaces exhibited better performance than nanospheres for highly sensitive DNA detection assay because of the faster DNA binding kinetics, sharper DNA melting transition and wider "hotspot" regions [110]. Another example to detect cancer biomarker is

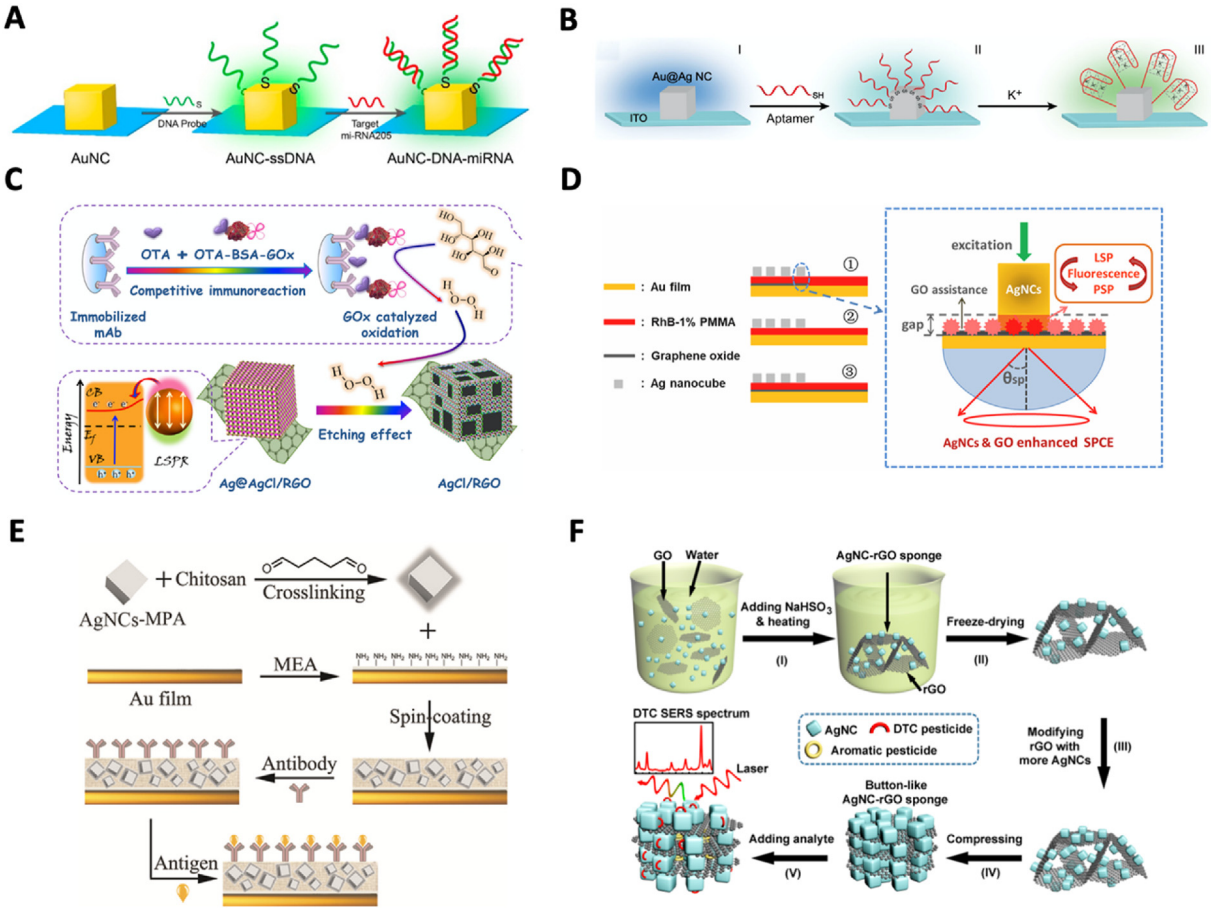

Fig. 8. Biosensors with plasmon assisted metal nanocubes. **A**. Au nanocubes which are modified by thiolated ssDNA. Replicated with permission from Ref. [57]. **B**. A plasmonic aptamer sensor on a single Au coated Ag nanocube. Replicated with permission from Ref. [58]. **C**. A plasmon enabled ochratoxin A (OTA) biosensor. Replicated with permission from Ref. [59]. **D**. A plasmonic sensor where Ag nanocubes are loaded on GO on Au films. Replicated with permission from Ref. [112]. **E**. A novel biosensor based on SPR with enhanced sensitivity using Ag nanocubes/chitosan composite. Replicated with permission from Ref. [60]. **F**. A SERS based sensor to detect dithiocarbanmate (DTC). Replicated with permission from Ref. [61].

presented by Li et al. [111] using the gold-silver alloy nanoboxes. With the strong Raman signal enhancement capability, the reported alloy nanoboxes combined with nanoyeast single-chain variable fragments show high sensitivity and specific capture performance. The researchers successfully detect three different soluble cancer protein biomarkers (sPD-1, sPD-L1, sEGFR) with a limit of detection of 6.17 pg/mL, 0.68 pg/mL, and 69.86 pg/mL, respectively. The detection of the three cancer protein biomarkers is also validated in human serum samples and achieved high recovery rates.

Tian et al. [58] fabricated a simple and sensitive plasmonic aptamer sensor on a single Au coated Ag nanocube, used its LSPR effect to analyze K^+ ions, and monitored the formation of G-quadruplex structure in real time. In this design, an ssDNA with G-rich specific sequency providing K^+ bonding site is bonded to the surface of the Au@Ag nanocubes as shown in Fig. 8B. This work showed that LSPR can provide an efficient tool for monitoring the interaction of K^+ ions with a range of 1×10^{-9} - 1×10^{-2} M and a limit of detection of 1×10^{-9} . M. Tang et al. [59] constructed a photoelectrochemical immunosensing platform using Ag@AgCl nanocubes decorated on reduced graphene oxide (RGO) heterostructure. RGO nanosheets serves as the substrate for Ag@AgCl nanoparticle are used for their improved charge separation and transportation. The device is fabricated by a sacrificial salt-crystal-template procedure followed by an ethylene glycol assisted reduction reaction. In their study, Tang and coworkers observed that glucose oxidase oxidation generates H_2O_2 which have etching effect on Ag nanocubes. The etching of the Ag material can be quantified via measuring the photocurrent. Therefore, they use this phenomenon as a new mode of signal detection and designed the plasmon enabled ochratoxin A (OTA) biosensor with the structure aforementioned which showed high sensitivity, low limit of detection and good reproducibility which can be ascribed to the role of LSPR (Fig. 8C). Xie et al. [112] investigated the plasmonic enhancement of the sensor based on Ag nanocubes loaded graphene oxide (GO) (Fig. 8D). In their study, they fabricated a plasmonic sensor where Ag nanocubes are loaded on GO on Au films. The enhancement is studied and via modeling the EM field patterns using FDTD solutions software (Lumerical Solutions). The found that the high EM field of Ag nanocubes, the localized surface plasmons (LSP) and the propagating surface plasmons (PSP) are responsible for the over 30 enhancement factors. Zhang et al. [60] fabricated a novel biosensor based on SPR with enhanced sensitivity using Ag nanocubes/chitosan composite. They synthesized Ag nanocubes using sulfide-mediated method. Au film is used as the substrate for the spin-coated Ag nanocubes/chitosan composite. The schematic of the device is shown in Fig. 8E. They attribute the enhancement in SPR response to the electronic coupling of the Ag nanocubes and the plasmonic surface waves. The biosensor demonstrated by detecting the IgG of mouse. In the experiment, the device showed a large detection range from 0.6 to 40 μg mL^{-1}. Zhang and coworkers reported an electrochemiluminescence sensor enabled by surface plasmon coupling effect on Au nanocubes. The found this effect is particularly strong on the apexes and edges of the Au nanocubes. Graphite phase carbon nitride quantum dots are used to further enhance the surface plasmon coupling effect, and as a result, the signal has been increased three times. In addition, toehold-mediated strand displacement, a simple and enzyme-free strategy, is employed to amplify the nucleic acid. The biosensor can detect rapidly accelerated fibrosarcoma B-type (BRAF) gene with a range of 1 pM to 1 nM and a limit of detection of 3.06×10^{-5} nM. Zhu et al. [61] developed a SERS based sensor to detect dithiocarbanmate (DTC), a pesticide, using sponge like RGO wrapped Ag nanocubes. As shown in Fig. 8F, layers of porous RGO sheets form a scaffold structure to hold Ag nanocubes. Adjacent Ag nanocubes contribute to the "hotspot" for the amplification of SERS signal. The sensor's selectivity of DTC is owing to the pesticide's preferential adsorption on the Ag surface and aromatic pesticides on the RGO surface. The detecting concentration ranges from 50 nM to 2 μM, and the limit of detection are 10–16 ppb.

Nanocubes can be applied to directly capture virus. A team has been working on the detection of norovirus using molybdenum and silver nanotubes by SERS. These nanocubes were functionalized with norovirus-specific antibody so that a core-satellite immunocomplex can be formed through antigen-antibody immunoreaction [113,114]. This detection sensor was characterized with a broad linear range from 10 fg/mL to 100 ng/mL and a limit of detection of ~0.1 fg/mL.

3.3. Spike/star

In addition to spherical and cubic shapes, AuNPs can be synthesis into star or spike shapes or similar shapes with sharp vertices [115]. For the first time, Au nanostars (Fig. 9A) were used in an assay for DNA detection based on selective capturing of DNA targets [62]. It is found that the electrical field enhancement at the nanostar tips contribute to the coupling of the LSP and surface plasmons. This bioprobe can detect unamplified human genomic DNA extracted from lymphocytes with a sensitivity down to 10 aM. Chatterjee and co-workers [116] developed a high-yield synthesis for fabricating Au nanostars with just one step. These nanostars have longer and sharper spikes which contribute to stronger "hotspot" at the spike tips. They also employed numerical tools to quantify the local electric field enhancement and LSPR. The single molecule SERS enhancement factor was found to be 10^{10} to 10^{13} in the calculation of optical simulation. Reyes et al. [63] developed a SERS based label-free method that utilize protein-induced aggregation of colloidal Au nanostars for rapid detection of enterovirus 71 (EV71) without substrate and laborious sample handling (Fig. 9B). Ahmed et al. reported a self-assembled Au nanostar based chiroimmunosensor for virus detection, specifically, avian influenza A (H4N6) [64]. They synthesized AuNPs into four different morphologies, namely, prolate-shaped, dendritic-shaped, flower-shaped and spiky-like AuNPs. The detection performance of these AuNPs is compared in the test of detecting influenza A virus (Fig. 9C). It is shown that the detection ranges are heavily dependent on the shapes of the AuNPs. Dr. Hamad-Schifferli and her research group developed a SERS based multiplexed assay that can distinguish between Zika and dengue, mosquito-borne diseases which have similar symptoms but may result in greatly different health outcomes [65]. This assay is designed to be a POC biosensor in which Au nanostars are conjugated to specific antibodies for Zika and dengue and employed in a dipstick-format immunoassay. The viral nonstructural proteins (NS1) from dengue and Zika are used as biomarkers. The immunoassay consists of a nitrocellulose strip on which NS1 antibodies are immobilized on the test line and a control antibody at the control line. Fig. 9D shows the immunoassay's schematic. To reduce time-to-result on a single platform without additional labeling and immobilization, a team reported an Au nanospike biosensor composed of DNA to achieve three functions at one time - target recognition, signal amplification, and connection to substrate [117]. They introduced DNA 3-way junction on the surface of Au nanospikes for protein recognition aptamer, FAM dye and immobilization thiol-group, respectively. A SERS based bioprobe was reported by Wang et al. that can image and biosense hypochlorite (ClO^-) and glutathione (GSC) [66]. 4-mercaptophenol (4-MP)-functionalized Au nanoflowers are fabricated and used to provide a large amount of "hotspots" to increase the SERS signals. The biosensor's working mechanism is shown in Fig. 9E. As a result, the limit of detection of the biosensor can achieve 0.38 and 0.4 μM for GSH and ClO^-, respectively. More recently, a new method is proposed to fabricate scaled-up, reproducible plasmonic biosensor which include a large number of "hotspots" for greatly enhanced detection capabilities [67]. In this design as shown in Fig. 9F, Au are made into nanopillars arrays by depositing AuNPs on a plasma-etched PET substrate via a vacuum process. The enhancement was found to be over 8.3×10^8-fold for SERS and 270-fold for plasmon enhanced fluorescence due to the high density of plasmonic coupling and quantity of "hotspot" in this design. The biosensor is able to detect influenza related antibodies with high sensitivity. This fabrication technique, which is simple and highly scalable, provide new avenues to facilitate mass production for POC plasmonic biosensors.

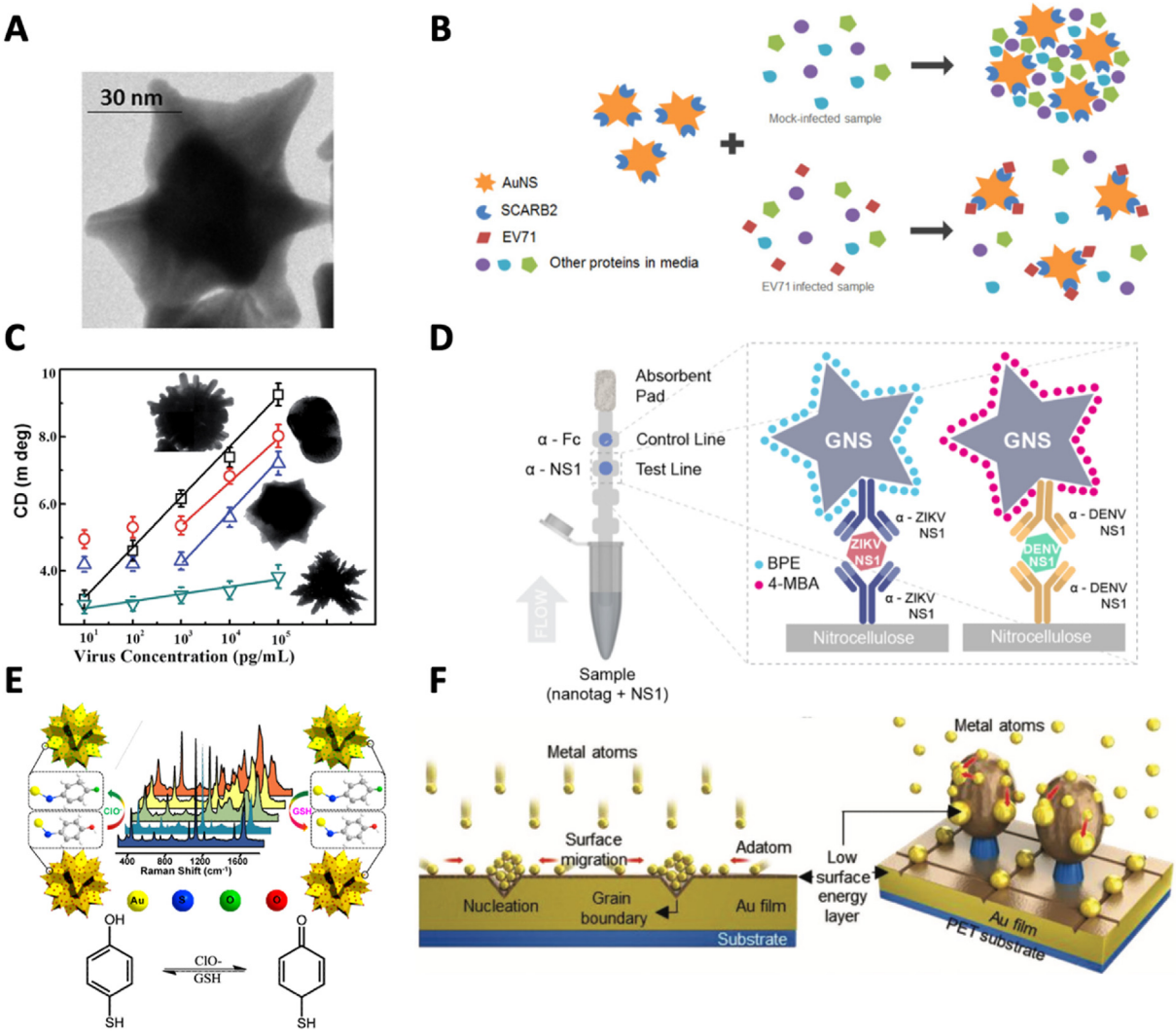

Fig. 9. Spike/star shaped AuNPs based plasmonic biosensor. **A**. The DNA detection using Au nanostars. Replicated with permission from Ref. [62]. **B**. A SERS based label-free method that utilize protein-induced aggregation of colloidal Au nanostars for rapid detection of EV71. Replicated with permission from Ref. [63]. **C**. A self-assembled Au nanostar based chiroimmunosensor for virus detection. Replicated with permission from Ref. [64]. **D**. A SERS based multiplexed assay that can distinguish between Zika and dengue. Replicated with permission from Ref. [65]. **E**. A SERS based bioprobe that can image and biosense hypochlorite (ClO^-) and glutathione (GSC). Replicated with permission from Ref. [66]. **F**. A scaled-up, reproducible plasmonic biosensor that include many "hotspots" for detection enhancement. Replicated with permission from Ref. [67].

4. Sandwich-, chip-, and paper-based designs

Immobilizing nanoparticles onto solid substrates provides higher flexibility, robustness, and easy application to plasmonic sensing, especially when applying non-water-soluble molecules [118]. This section reviews three major sensing platform structures, namely, sandwich-, chip-, and paper-based designs for plasmonic biosensing. Silicon has been used as a traditional substrate for nanoparticle immobilization for years due to the well-developed nanofabrication methods, such as e-beam lithography [119,120], charged particle beams [121] and thermal evaporation [122], to precisely control the size, shape and density of deposited nanoparticles. For instance, Bibikova presented a straightforward method to produce SEIRA- and SERS-active substrates based on the plasmonic properties of wet-chemically synthesized AuNSts, which were subsequently immobilized at silicon chips mediated by a gold layer and α-ω-dimercapto polyethylene glycol [123]. The advantage of nanoparticle deposition at the silicon surface is their strong adhesion at the gold-coated silicon interference. This property significantly improves the stability of the obtained AuNP modified Si substrates, which allows reusability after cleaning.

4.1. Sandwich structure

Immunoassays typically include two modes: competitive and noncompetitive assays. In competitive assays, unlabeled antigen in the test samples competes with prelabeled antigen to bind the antibody. When the amount of antigen in the test sample increases, the detected signal measured from the labeled antigen typically decreases. As a result, competitive assays need to have a strong detected signal for the labeled antigen [124,125]. The other mode is the noncompetitive immunoassays, which typically combine a primary antibody for immobilization and a secondary antibody for signaling. Since analyte is bonded between two antibodies, this type of assay is also known as the sandwich-type assays. The measured signal is directly proportional to the concentration of analyte, and this type of assay has very high sensitivity.

For decades, sandwich-structured biosensors have been intensively developed for disease diagnosis. The most commonly used sandwich immunosensor is the AuNPs/antigen/AuNPs where AuNPs are conjugated with different antibodies for different detection purposes. For example, Kim et al. [126] developed a heteroassembled AuNPs sandwich-immunoassay LSPR chip for detection of hepatitis B surface

antigen, which is shown in Fig. 10A. The HBsAg were captured on AuNPs arrayed on glass substrate, and the captured HBsAg were further conjugated with a layer of AuNPs for signal amplification. The gold nanoparticles were fabricated through a classic seed growing method. This platform is able to detect HBV with a LOD of 100 fg/mL in 10–15 min, which satisfies the rapid and sensitive requirements of POC diagnosis. These results were validated in spiked human serum samples. Similar AuNPs/antigen/AuNps sandwich-structured immunosensors include the detection of ManLAM (Tuberculosis biomarker) with SERS by Crawford et al. [127], detection of SARS-Cov-2 Virus (COVID 19 protein) with SPR by Das et al. (Fig. 10B) [128] and the detection of thrombin by Lee [129].

In immunoassays, one of the key challenges is to enhance the plasmonic signal. For this purpose, different signaling markers have been employed in the sandwich immunoassays. For example, Zou et al. [130] developed a sandwich-structured immunosensor to detect Tuberculosis with magneto-plasmonic nanoparticles (MPN) (Fig. 10C). In this platform, antigen was captured on a gold chip and conjugated with Fe_3O_4@Au nanoparticles for enhanced signaling. Zou et al. fabricated Fe_3O_4@Au core-shell nanoparticles in three different morphologies (i.e., sphere, short spiky and long spiky) to amplify the SPR signals and found spherical MPN can enhance the electronic coupling effect significantly, showing the best detection sensitivity. Their system was able to detect CFP-10, which is an early secretary antigen of Tuberculosis, with a LOD of 0.1 ng/mL. The developed immunosensor was evaluated in artificially CFP-10-containing urine which are easy to collect. In another study from Zhang et al. [131] they form the sandwich sensor by using IRDye800 fluorophore to label the captured antigen on the plasmonic Au substrate for the detection of type 1 diabetes. Li et al. [132] also employed IRDye800 fluorophore in their sandwich sensor for labeling (Fig. 10D). However, Li et al. developed this platform not to detect an already-known disease biomarker, but to profile the autoantibodies that are related to hypertensive heart disease. Through evaluating the detected cardiovascular autoantibodies, autoantibodies to troponin I, annexin-A5, and ADRBK1 emerged as the most strongly associated with LV remodeling and dysfunction in patients with hypertension.

4.2. Microfluidic chip

Being the technique to precisely manipulate fluids at the microscale, microfluidic technology is capable of implementing bioreaction with minimized reagent and shortened span, thus can significantly reduce the cost and time of detection [24–26]. Compared with traditional platforms, integrating microfluidic systems with plasmonic microsensors offer a bunch of advantages in cost, sensitivity, and adaptability. Microfluidic chips are typically fabricated in a simple and reproducible approach with low cost, which are suitable for fabrication with batch mode in clinic. In the meantime, microfluidic reactors enable homogeneous and thorough reaction with reduced specimen, thus increasing the sensitivity and accuracy of detection. Further, microfluidic chips are versatile and can be easily adapted for various purposes, such as automated measurements, connection to other instruments, and label-free sensing. Low cost, portable device, high throughput, high sensitivity, rapid reaction, simplified steps, all of which outstanding characters indicate that microfluidic-based plasmonic sensing platforms are ideal for POC disease diagnosis [133,134].

Thanks to the high throughput, microfluidic chips can generate a well-defined detection environment for plasmonic sensing systems. Mühlig et al. [135] set up a droplet-based lab-on-a-chip device to detect mycobacteria using SERS. In this platform, bacteria were disrupted and pumped into the microfluidic channel together with the fabricated Ag nanoparticles to record the LOC-SERS spectra. The droplet-based microfluidic device can analyze a large number of independent samples rapidly with low sample volume, thus can conveniently generate a statistical valid data set for detection. However, this system still requires a Raman microscope to do the measurement, which limits the application scenario. Other researchers incorporate microfluidic devices with plasmonic sensors to introduce a fast and portable detection method [136–139]. For example, Yap et al. [136] presented a novel bifunctional microfluidic SERS immunoassay with plasmonic-magnetic nanoparticles. In the immunoassay, plasmonic nanoparticles act as soluble SERS immunosubstrates and magnetic particles promote micromixing,

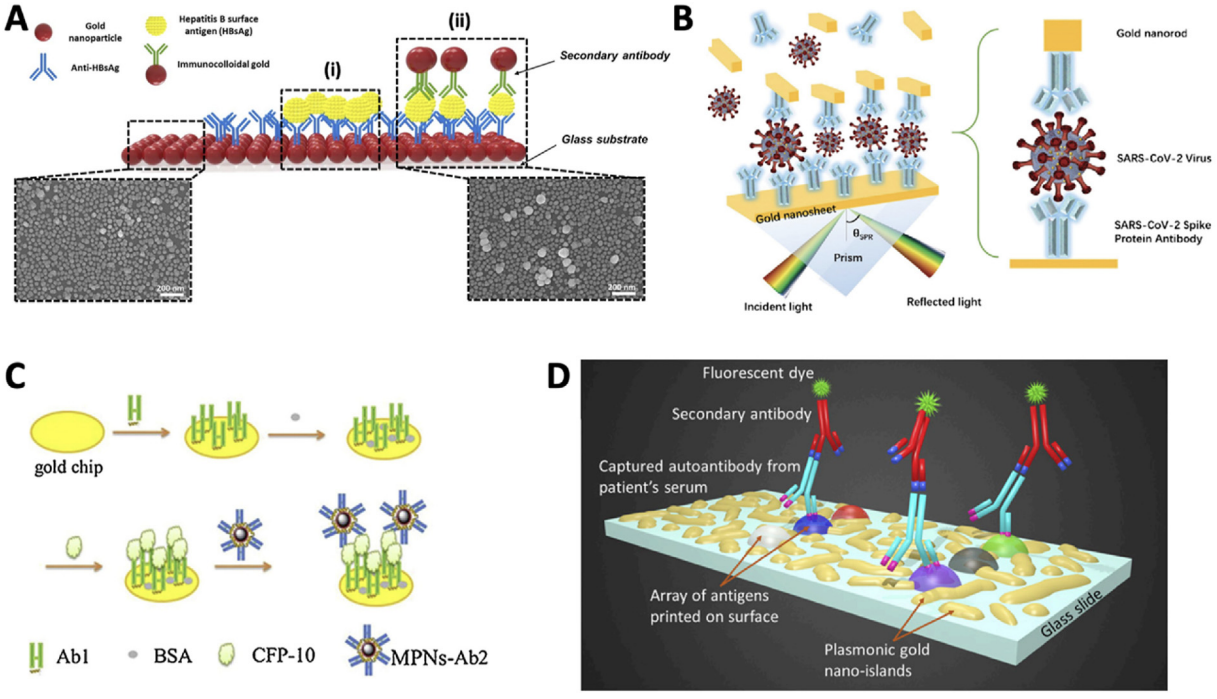

Fig. 10. Scheme of sandwich-structured biosensors for diagnosis. **A**. The heteroassembled AuNPs sandwich immunoassay LSPR chip to detect HBV. Replicated with permission from Ref. [126]. **B**. The structure of the gold nanorod assisted plasmonic immunoassay for detection of COVID-19 SARS-CoV-2 Spike Protein. Replicated with permission from Ref. [128]. **C**. The magneto-plasmonic nanoparticles enhanced SPR chip to detect Tuberculosis. Replicated with permission from Ref. [130]. **D**. A plasmonic sandwich microarray structure to detect cardiovascular diseases. Replicated with permission from Ref. [132].

together yielding a rapid detection in a simple device. Zhou et al. [137] built up a cost-effective plasmonic immunochip for the detection of carcinoembryonic antigen (CEA) by integrating plasmonic sensing with microfluidics and nanoimprint lithography (Fig. 11A). Plasmonic nanocave array with excellent bulk refractive index sensitivity is implemented in the platform to provide stable functionality and simple measuring configuration. This chip achieves detection capability for the CEA concentration of less than 5 ng/mL within 30 min, which is much lower than the CEA cancer diagnosis threshold of 20 ng/mL. Vazquez-Guardado et al. [138] developed a plasmonic sensing system to directly detect neurotransmitter dopamine from whole blood (Fig. 11B). The microfluidic separator enables in-line separation of plasma directly from the bloodstream and channels it to the detection area coated with inorganic cerium oxide nanoparticles for rapid detection. The platform achieves detection of dopamine at 100 fM concentration in simulated body fluid and 1 nM directly from blood. In the following year, Inci et al. [139] reported a disposable hand-held microfluidic plasmonic platform to detect hemoglobin protein. With the capability to finish the typical assess in 15–30 minutes for end-users, this cost-effective miniaturized chip shows great potential in POC applications. At the meantime, microfluidic devices are easily to be designed with parallel microchannels, which allows for parallel detection of multiple antigens [140,141] An example was presented by Geng et al. [140] with an optofluidic-portable platform to integrate LSPR spectroscopy and microfluidic technology to deliver a low-cost, ultra-sensitive detection system for liver cancer antigen (Fig. 11C). The vacuum evaporation followed by thermal annealing method was used to fabricate the AuNPs on microfluidic chip. This chip contains 9 cells and is connected to optical probe and data handling system to allow for parallel in-situ test and real-time measurement. Soler et al. [141] also reported a nanoplasmonic microfluidic biosensing system that can do simultaneous detection of two bacterial infections: *Chlamydia trachomatis* and *Neisseria gonorrhoeae*. This system introduces precise immobilization of specific antibodies on the individual sensor arrays for selective detection and real-time quantification with a limit of detection of 300 CFU/mL and 1500 CFU/mL for the o bacteria respectively. Peláez et al. [142] combined the SPR gold chip with microfluidics to realize POC for tuberculosis diagnosis. The presented biosensor is functionalized with highly specific monoclonal antibodies, allowing for detection and quantification of the heat shock protein X (HspX) directly in pretreated sputum samples. Microfluidic plasmonic sensing system offers new solutions for the current COVID-19 pandemic. Funari et al. [143] developed an opto-microfluidic chip for the detection of antibodies against SARS-CoV-2 spike protein by gold nanospikes. The microfluidic chip is covered with functionalized Au nanospike and combined with a homemade reflection probe to collect the reflective light to record and process the absorbance spectrum. Funari et al. showed that this opto-microfluidic platform can detect the target protein in diluted human plasma within 30 minutes and achieves an LOD of ~ 0.08 ng/mL.

4.3. Paper based design

Paper-based sensing platforms have attracted increasing interest and obtained rapid development in the past few years since Whitesides et al. first introduced the potential of microfluidic paper-based analytical devices (μPADs) in 2007 [144]. With the advantages of low-cost, widespread availability of material, facile manufacture, high biocompatibility and ease of use, paper-based devices is becoming ideal platforms for POC diagnosis applications. Paper-based devices are typically composed of hydrophilic or hydrophobic microstructures patterned on the paper substrate to allow for capillary-driven flow. These paper-based devices are usually fabricated through wax printing [145], inkjet printing [146], screen printing [147], photolithography [148] and plasma treatment [149].

Paper-based devices can be easily combined with the colorimetric detection method to provide fast and cheap diagnosis through visual readout without handling other tools or apparatus. In colorimetric assays, the reagents are first loaded to the paper substrate and will be later interact with the analyte solution to create a visible color change in the paper. For example, Fakhri et al. [150] developed a novel paper-based biosensor to detect concentrations of miRNA-21 in human urine

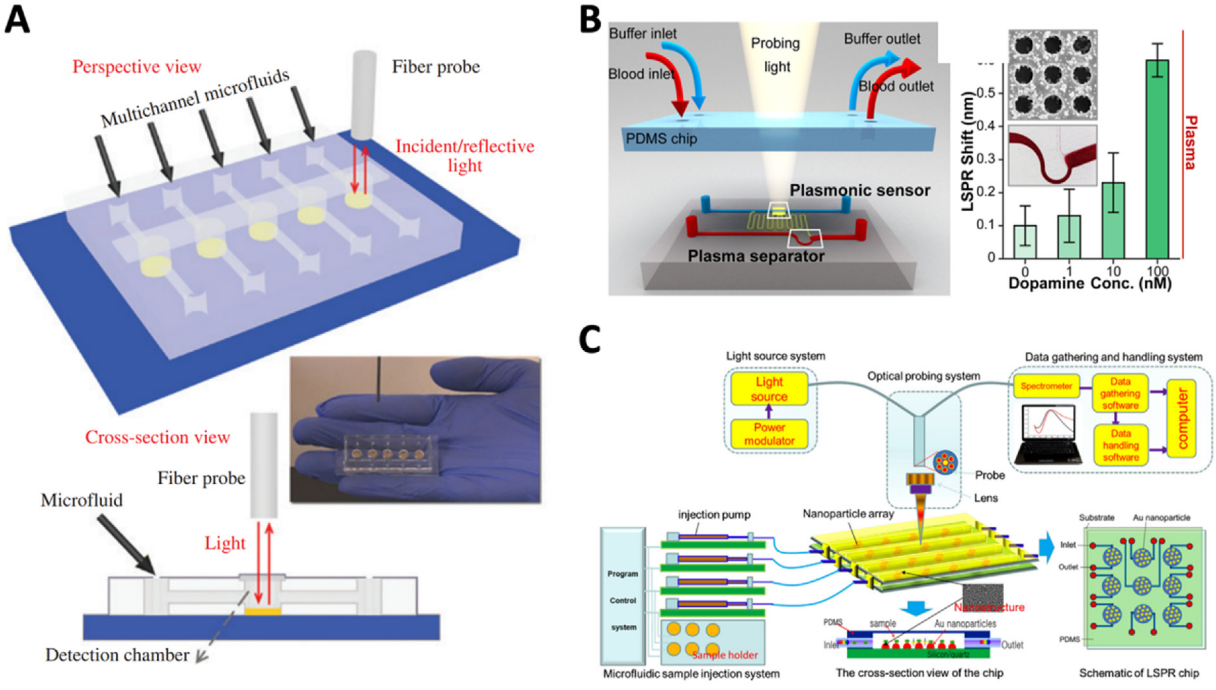

Fig. 11. Microfluidic plasmonic sensing platforms. **A**. A microfluidic immunochip with plasmonic gold nanocave array and a fiber probe for tumor detection. Replicated with permission from Ref. [137]. **B**. A microfluidic separator embedded with plasmonic sensor to directly detect neurotransmitter dopamine from whole blood. Replicated with permission from Ref. [138]. **C**. An optofluidic biosensor platform integrated microfluidics and LSPR sensing chip. Replicated with permission from Ref. [140].

sample. This biosensor is incorporated with DNA-templated Ag/Pt nanoclusters to catalyze the reaction of hydrogen peroxide and 3, 30, 5, 50 tetramethylbenzidine (TMB) to produce a blue color. This biosensor is able to reach a detection limit of 0.6PM with a large linear detection range. Another example is presented by Srisa-Art et al. [151] to detect Salmonella typhimurium using paper-based device (Fig. 12A). IMS anti-Salmonella coated magnetic beads are applied to capture and separate the bacteria from sample, followed by the implementation of a sandwich immunoassay for the detection. The concentration of Salmonella typhimurium can be read as the length of colored band and reach a detection limit of 10^2 CFU mL^{-1}. Instead of using simple piece of paper, Son et al. [152] show the potential of PDA-paper in the immunoassays to detect the high infectious pH1N1 virus among influenza A viruses (Fig. 12B). Their colorimetric sensor employs PDA-paper chip as the substrate, which exhibits blue-to-red colorimetric transitions upon environmental change. Conjugated with antibody, the PDA-paper chip is able to detect pH1N1 virus with visible color change. Other researchers also use paper-based colorimetric immunosensors to detect different irons which are toxic to human beings, including lead ions [153] and mercury ions [154].

It is worth noting that paper-based colorimetric immunosensors usually have low sensing signal, which can often limits their application in the disease diagnosis. To amplify the sensing signal of paper-based sensors, Alba-Patino et al. [155] developed an origami paper-based colorimetric biosensor with decreased detection limit. By simply folding a piece of paper as substrate and loaded with conjugated gold nanoparticles, the immunosensor can generate simultaneous visualization of colorimetric signals in each layer of paper (Fig. 12C). Due to the semitransparent nature of wet paper, signals are added layer upon layer to form higher optical density. It is showed that the limit of detection is decreased 10 times in a model immunosensor for the detection of immunoglobulins.

Paper-based devices also show great potential in SERS. Traditional SERS immunosensors are fabricated by generating metal nanostructures on the substrate, which is typically done by sophisticated and expensive deposition technology. Compared with traditional substrate material such as silicon wafer or glass, paper has cellulose structure to directly absorb the reagent via spotting and can even form a higher Raman enhancement factor [156]. The theme of flexibility, low cost and high sensitivity can be reflected in many recent studies. For example, Oliveira et al. [157] decorated office paper with silver nanostars to obtain increased SERS sensibility, high uniformity and reproducibility (Fig. 12D). Moram et al. [158] fabricated a SERS platform by employing filter paper embedded with salt-induced aggregated Ag/Au nanoparticles and validate their application to detect multiple explosive molecules. Hu et al. [159] constructed a uniform paper-based SERS test strip via *in situ* synthesis of AuNPs on paper fibers for the detection of Mucin-1 in whole blood. Lee et al. [160] reported a filter paper based SERS sensor which is hydrophobic modified by alkyl ketene dimer for the detection of pesticide with sub-nanomolar sensitivity. In addition to paper-based devices, we have summarized a list of other non-metal based plasmonic devices in Table 2. A commonly used materials is graphene that is proven to increase the sensitivity of plasmonic detections [161]. These nonmetal based devices' synthesis and working method, their target disease and biomarkers, evaluation of potential POC feasibility, and limit of detection are also summarized and compared.

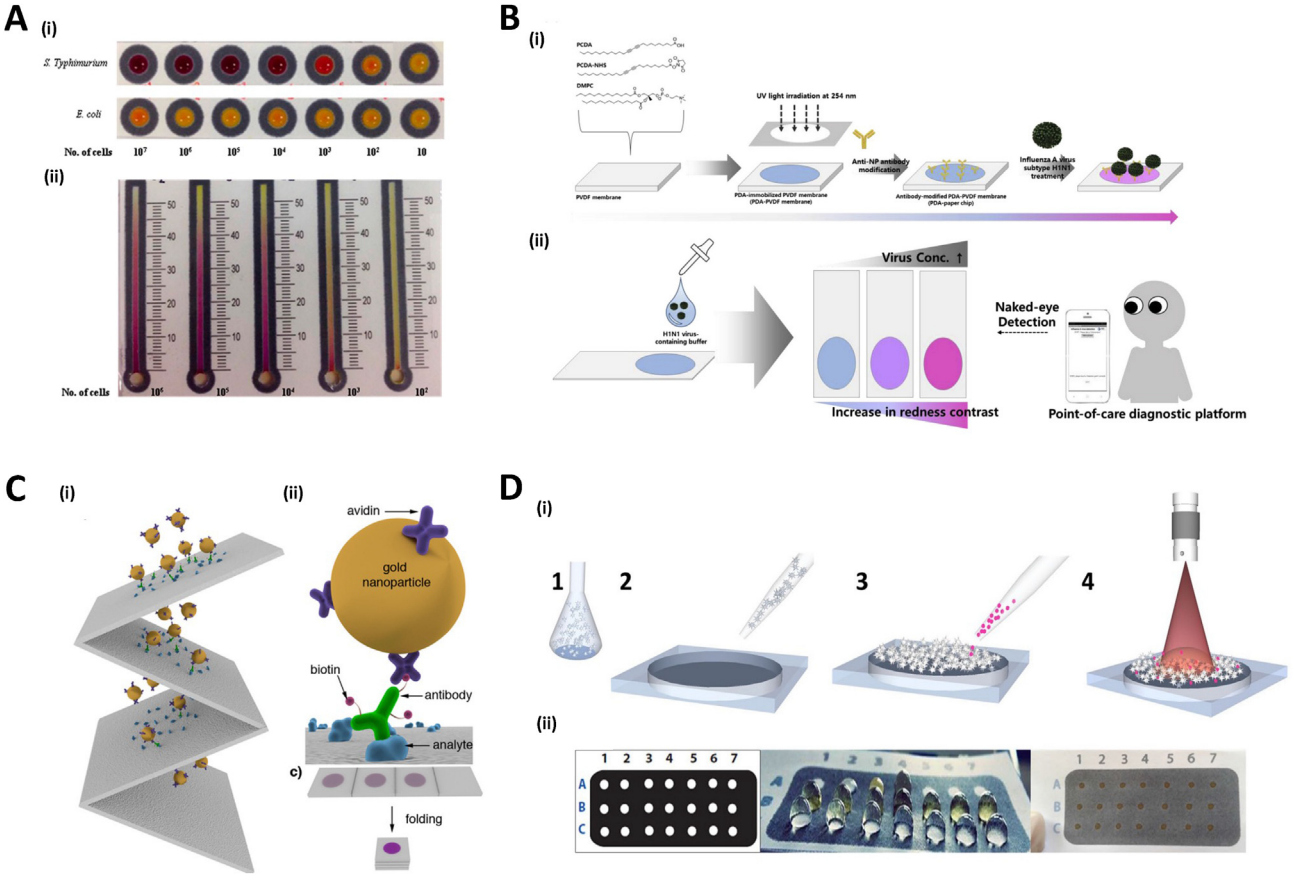

Fig. 12. Examples of paper-based immunosensors. **A**. The readout results from colorimetric paper-based sensor to detect Salmonella typhimurium. Replicated with permission from Ref. [151]. **B**. Preparation of PDA-paper chips and their application for the colorimetric detection of influenza A (pH1N1) virus. Replicated with permission from Ref. [152]. **C**. Schematic representation of the origami paper-based biosensor. Replicated with permission from Ref. [155]. **D**. The fabrication process and pattern design of the office paper based plasmonic SERS substrates. Replicated with permission from Ref. [157].

Table 2
Summary of examples of nonmetal based plasmonic biosensors.

Materials	Synthesis method	System/Method	Disease detected	Biomarker	POC ability	Limit of detection	Ref.
RGO	Sputter coating (Au) incubated with RGO	SPR	Dengue	DENV 2 E-proteins	High	0.08 pM	[162]
Paper	Commercial product (Dynabeads, streptavidin−β-galactosidase conjugate)	Colorimetric sensing	Salmonellosis	Salmonella typhimurium	High	100 CFU/mL	[163]
	Photo irridation (PDA)	Colorimetric sensing	Influenza A	pH1N1	High	10^3–5×10^3 $TCID_{50}$	[164]
Polymer	Polymerization	SPR	HBV	Anti-HBs	High	N/A	[165]
Graphene	Commercial product (Graphene)	Colorimetric	Inflammation	C-reactive protein	High	0.07 ng/mL	[166]

5. Meta-surface patterned design

This section reviews and discusses research efforts made towards the patterning of surfaces with plasmonic structures for large-scale surface-based sensors [167]. Table 3 summarized some recently developed, representative examples of plasmonic biosensors based on patterned meta-surface and nanoarray structures that enhance the plasmonic effect. Their synthesis and working method, their target disease and biomarkers, evaluation of potential POC feasibility, and limit of detection are also summarized and compared. This section will cover three main classes within this field, discussed in increasing levels of scalability, namely lithographic patterning, nanoisland films, and finally chemical growth (Fig. 13).

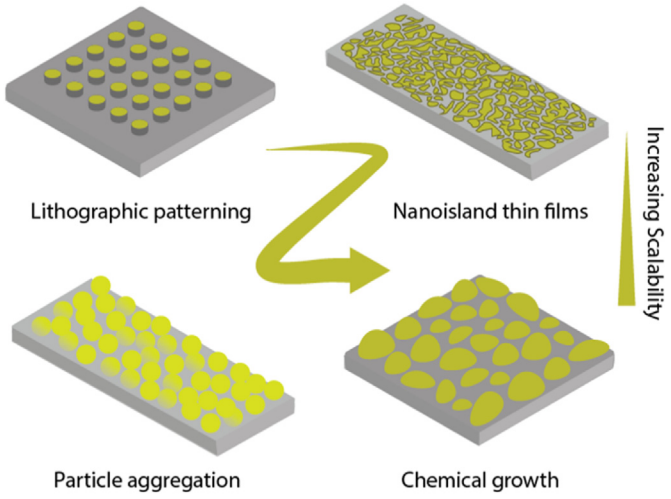

Fig. 13. Overview figure showing the various techniques used for patterning of surfaces, namely, lithographic patterning, nanoisland thin films, particle aggregation, and chemical growth.

5.1. Lithographic Patterning

Lithographic patterning of metallic films for the creation of plasmonic nanostructures is a commonly utilized approach that allows for unparalleled levels of tunability and control. By virtue, such systems often achieve the highest levels of enhancement of the techniques that will be discussed herein. However due to lack of scalability of many of the techniques used, these configurations have not found significant translation to POC applications. Due to the size of the desired structures, electron-beam lithography is often required for their fabrication, creating further limitations in terms of scalability and time of processing. In its most basic form, this technique requires the spin coating and patterning of a photoresist film via electron-beam writing. Following pattering, the photoresist can be developed removing the unwanted areas after which metallic thin films can be deposited and the remaining resist removed via a lift-off process. Due to the use of an electron-beam, the resolution of this technique allows for the writing of nanoscale features and highly controlled geometries benefiting performance. Using this approach, an early demonstration of plasmon-enhanced fluorescence was shown, with fluorescence enhancement of up to 1000-fold demonstrated experimentally [32]. Alternatively, more scalable and wafer-scale lithographic processes have been developed using variations of more standard traditional ultraviolet lithography. In one example, a modified deep UV lithographic process was used to create wafer scale plasmonic nanohole array geometries [181] (Fig. 14A). This system was coupled with gold nanoparticles which when bound to the nanohole array reduces the transmission at the resonance wavelength of the nanohole array. The

Table 3
Summary of examples of meta-surface and nanoarray based plasmonic biosensors.

Surface form	Synthesis method	System/Method	Disease detected	Biomarker	POC ability	Limit of detection	Ref.
Meta-substrate	Commercial product (Au), magnetic sputtering method	Plasmonic fluorescence	Cardiac disease	Cardiac troponin I	High	0.01 ng/mL	[168]
	Commercial product (Au)	SPR	TB	DIG	High	63 pg/mL	[169]
Meta-coated slides	Sputtering (Au)	SPR	Dengue	DENV-2 E-proteins	Low	0.08 pM	[170]
	Seed-mediated growth on glass slide (Au)	Plasmonic fluorescence	Diabetes	Islet cell–targeting autoantibodies	High	N/A	[171]
	Commercial product (Au)	SPR	Cardiac disease	Cardiovascular autoantibodies	Medium	N/A	[172]
	Thermal annealing (Ag)	LSPR	Dengue	Dengue NS1 antigen	High	9 nm/(μg/mL)	[173]
	Evaporation (Au)	SPR	Cancer	Carcinoembryonic antigen	High	5 ng/mL	[174]
	Electron beam evaporation, thermal annealing	LSPR	Liver cancer	Liver antigen, liver antibody	High	Antigen 45.24 ng/mL Antibody 25 ng/mL	[175]
	Coating Au on butterfly wings	SERS	Malaria	Malarial hemozoin	Low	N/A	[176]
Nanoarray	Tetrahedron DNA monomers	SPR	HIV	HIV-related DNA	High	48 fM	[177]
	Commercial product (Spreeta 2000 chip)	SPR	TB	Ag85	High	10 ng/mL	[178]
	Commercial product (Au)	SPR	Ebola	mAb1, mAb2, mAb3	Medium	0.5 pg/mL	[179]
	Seed-mediated growth on glass slide (Au)	SPR	Diabetes	ZnT8A	Low	N/A	[180]

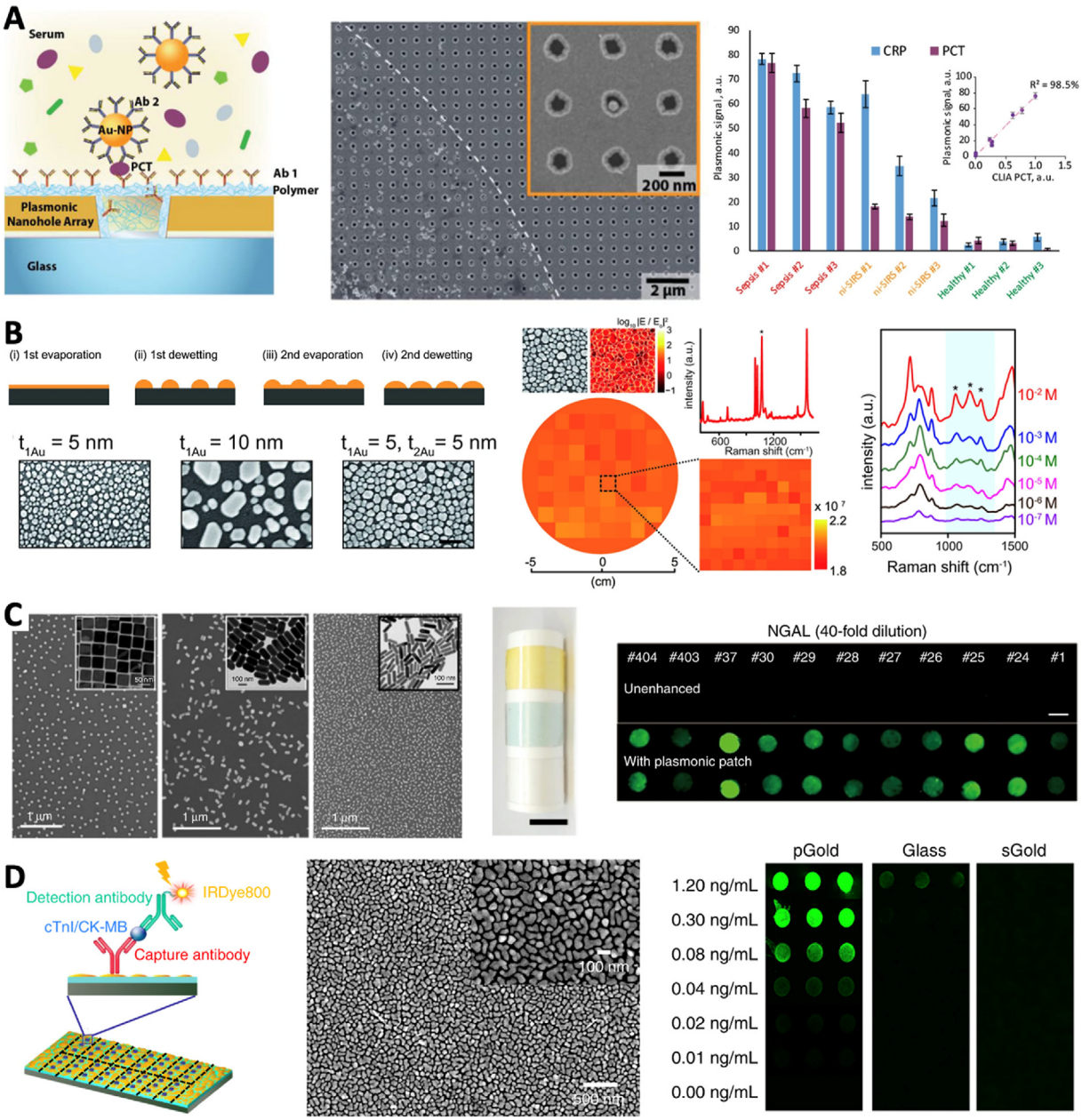

Fig. 14. Overview of patterned plasmonic surfaces. **A**. A nanoplasmonic array fabricated using lithographic methods, which utilizes extraordinary transmission demonstrated by the structure for the sensing of captured analytes then applies this for sepsis diagnosis using two widely accepted sepsis-related biomarkers, CRP and PCT. Replicated with permission from Ref. [181]. **B**. A repeated thin film dewetting process to form densely packed particle arrays which exhibit significant Raman enhancement and was used in the detection of octopamine molecules. Replicated with permission from Ref. [188]. **C**. A nanoparticle deposition/aggregation using three different nanoparticle morphologies, their large-scale patterning potential using a polymeric surface, and their application within plasmon enhanced fluorescence applications. Replicated with permission from Ref. [2]. **D**. A solution-based synthesized microchip containing densely packed films and its application within plasmon-enhanced fluorescence application for the diagnosis of myocardial infarction. Replicated with permission from Ref. [194].

developed system was coupled with a portable optical reader which enables POC potential and results from the system could be ascertained within 15 min. As a use-case for the developed system, the group explored the detection of sepsis using two sepsis-related biomarkers, procalcitonin (PCL) and C-reactive protein (CRP), and showed limit of detection of 21 and 36 pg/mL, for each, respectively. Within a clinical cohort they demonstrated the ability to distinguish between sepsis, noninfectious sepsis, and healthy individuals (Fig. 14A). Though these results are promising and performance impressive, for use within the POC, scalability is a crucial concern and a shortcoming of lithographic methods.

5.2. Nanoisland films

The nanoisland film morphology has been a widely utilized configuration due to advantageous optical properties including enhanced field intensities resulting from closely packed yet isolated clusters of particles. This general morphology has been fabricated using two main methods, both involving first the deposition of metallic thin films. In the standard configuration of this morphology, highly controlled deposition of metallic film films prior to film percolation is completed (often <10 nm for gold thin films) [182–184]. High percolation thresholds due to atom mobility and surface tension results in gold thin films forming in a non-continuous sheet of closely packed though distinct island-like

clusters [185]. Due to the close-packed, yet distinct islands there exists significant interaction between adjacent "hotspots" leading to significant field enhancement [186]. As the film thickness grows, the film will become continuous and the advantageous optical properties diminish [187]. An alternative method in the fabrication of nanoisland-like geometry is thermal dewetting of gold thin films. In this case, the metallic thin film layers are heated to high temperatures and rearrangement of the gold particles occurs as the sheets undergo a dewetting process, resulting in the formation of nanoislands [188]. By altering numerous parameters within the process including the temperature, metallic thin film thickness, time of heating, among others, the level of rearrangement can be altered leaving to various characteristic morphologies [189–193]. One intriguing study within this field utilized repeated deposition and dewetting to increase the number of plasmonic "hotspots" and as a result the extinction intensity (Fig. 14B). This substrate was tested for SERS of octopamine molecules with a limit of detection of 10 μM for multi-step dewetting, compared to 100 μM for single-step detwetting [188]. Both pre-percolation films and thin film detwetting techniques introduced first require the step of metal deposition. However due to the thickness of the desired films and possibility for large-scale patterning, there is potential for such techniques to be useful for POC applications.

5.3. Chemical growth

Chemical growth is another means for the development of patterned plasmonic surfaces and has the highest potential for scalability to meet demands of POC assays. To promote the use for POC applications which necessitate scalability there has been a continual push in the field for simplistic fabrication mechanisms which omit the use of specialized equipment and processing such as that in lithographic processing and traditional nanoisland films. Arising from this work there has been a host of papers utilizing a simple yet highly effective technique in which chemically synthesized nanoparticles are bound onto a substrate forming a plasmonic surface which can be used directly within fluorescent assays, surface-enhanced RAMAN, LSPR, and the like [1,2,4,11]. In contrast to lithographic methods which allow for highly controlled patterning, within nanoparticle deposition/aggregation there exists no means to control where particles are patterned and particles are often suspended within a solution where incubation enables particle binding. By the nature of this process and the need for particle adsorption to the surface, this process is slow, yet due to the solution-based nature, can be highly scalable. A unique attribute of these systems is the ability to finely control the chemically synthesized particles prior to deposition thereby drastically altering the resulting films optical and plasmonic properties [1,2]. In one example of this system confirmation, three different particle geometries were explored, namely gold core silver shell nanocubes with an LSPR peak of 490 nm, and two gold nanorods with LSPR peaks of 670 and 760 nm, respectively, for use within plasmon-enhanced fluorescence applications (Fig. 14C). Particle aggregation was completed using a simple incubation process resulting in positively charged plasmonic particles absorbing to a negatively charged polydimethylsiloxane layer. Since spacing between fluorophore and plasmonic particles is critical to overall enhancement, following deposition, a polymer spacer was added via solution processing to enable a spacer layer between the plasmonic particles and nearby fluorophores [2]. As a use case, they tested this substrate for the detection of early-stage biomarkers or acute kidney injury, namely kidney injury molecule-1 and neutrophil gelatinase-associated lipocalin and showed 100-fold fluorescence enhancement over non-treated substrates (Fig. 14C).

In chemical growth, techniques common for solution-based synthesis of gold nanoparticles are modified and in turn can allow for the growth of particles upon a substrate. As is common within chemically synthesized particles, protocols of this nature typically include a seeding step followed by a growth step where the particle size can be tuned. Though, as of yet, this technique hasn't been able to show the breadth of morphologies and geometries able to be formed using standard solution-based chemical synthesis leading to lower levels of tunability, the application of these techniques to substrates has led to the creation of unique morphologies similar to the nanoisland-like films. Considering that fabrication occurs directly upon the desired substrate and that no specialized equipment is needed, fabrication can be highly scalable and rapid [187, 194–197]. Many of these structures have found use within plasmon-enhanced fluorescence and surface-enhanced RAMAN spectroscopy. Another unique attribute of chemical methods, is the ability to pattern alternative substrates, including polymeric surfaces. The earliest demonstration of this fabrication method was presented by Tabakman et al. [187], where full substrate synthesis could be completed in ~30 minutes of solution time, which included a three step process. Firstly, seeding of gold was completed upon the substrate by adding ammonium hydroxide into a chloroauric acid solution resulting in the precipitation of Au seeds upon the substrate of choice. Following seeding, reduction of the gold seeds was completed using sodium borohydride leading to the formation of Au^{3+}. Lastly, selective growth of seeds via hydroxylamine reduction in a chloroauric acid solution enabled reduction of Au^{3+} onto the seeds, forming nanoislands [187]. This initial paper further showed the feasibility for tuning structure by changing parameters including seed density and concentration of Au^{3+} during growth phase, altering optical properties. This substrate was later optimized and utilized for the diagnosis of myocardial infarction using the plasmonic nanoislands as a means for plasmon-enhanced fluorescence [194] (Fig. 14D), where it showed a diagnostic sensitivity of 100% and specificity of 95.54%. This study utilized cardiac troponin I, and showed dynamic range of 0.01–1.20 ng/mL and limit of detection as low as 0.0100 ng/mL, an 130-fold improvement over a substrate without nanoislands.

The three methods discussed herein describe the main methods presented thus far in literature for the patterning of substrates with plasmonic materials. Future efforts of this field should focus on the development of alternative fabrication mechanisms that emphasize scalability and portability to promote use within POC settings.

6. Challenges and perspectives

Despite the booming of development of nanomaterial based plasmonic sensors for POC applications in recent years, there remain many challenges at present and ahead. Among challenges the technologies are facing, we selectively discuss the ones that are most urgent. The first one is the Covid-19 global pandemic which requires rapid, POC diagnostic tool to quickly identify contraction of the virus. To develop reliable, accurate plasmonic sensing tools, machine learning assisted algorithms can serve as a fast and predictive tool to model the optical properties of nanoparticles. Miniaturization of sensing devices is also critical in facilitating the process of converting the current lab-based detection method to POC tools. Lastly, in disease detection, there exist many gold standards in clinical settings, to which many other innovative detection tools are compared including plasmonic sensing tools. In this section, we provide discussions and unique perspectives on these areas and hold a general belief that plasmonic diagnostic devices are able to cope with those challenges with future works.

6.1. Covid-19 testing

As of November 2021, there are approximately 250 million people worldwide who contracted Covid-19, a severe acute respiratory disease caused by coronavirus SARS-CoV-2, and 5.05 million people have died as a result, according to The New York Times and Johns Hopkins University. Regardless of the stages of this pandemic, the accessibility to Covid-19 test is critical. The tests have to be timely, easy, quick, and accurate in order for more people to get tested, which provides important information to governments and health agencies to contain the virus and drive the world to "new normal". During the pandemic, governments in many countries offered test sites where people can visit and get tested. However, problems like complicated registering process, long waiting times

and travelling to these sites remain hurtles that prevent many people from getting tested. Therefore, to solve this problem, scientists and engineers developed various types of POC biosensors that aim to provide rapid testing of coronavirus at one's own location, saving the time-consuming trip to go to a test site and providing an important tool to governments and health agencies to monitor the spread and progress of the highly contagious disease [198–200]. Plasmon enabled Covid-19 biosensors are one of the most promising tools to provide a POC solutions to Covid testing [201]. Djaileb et al. [202] developed a portable SPR based sensor for Covid-19 detection. In the design, the sensing chip's gold surface is modified with a monolayer of 3-MPA-LHDLHD-COOH which bonds with the SARS-CoV-2 nucleocapsid protein (rN). SPR shift is then observed and calculated as indicator for the existence of anti-rN antibody release by immune system in response to the SARS-CoV-2 virus. Qiu et al. [203] designed a biosensor that combines the plasmonic photothermal effect and LSPR mechanism. Au nanoislands are fabricated and functionalized with complementary DNA receptors. Selected sequences from of the SARS-CoV-2 virus can be detected through nucleic acid hybridization on the DNA receptors with a low limit of detection of 0.22 pM concentration. In addition to developing the above-mentioned Covid-19 sensor prototypes, researchers have also investigated the sensor using theoretical analysis and computational simulations in an effort to design an ideal Covid-19 sensor. Masterson et al. [204] reported a label-free plamonic nanosensor that can quantitatively detect 10 different biomarkers within one platform. The developed biosensor platform shows the capability to quantify IgG and IgM directly from COVID-19-positive patient plasma samples at the same time. Peng et al. [205] and Manas Das et al. [71] constructed models of near infrared SPR biosensor and plasmonic immunoassay, respectively, to explore the theoretical potentials of these sensors in POC coronavirus diagnoses. Moreover, rapid onsite detection is crucial to realize POC diagnosis. Li et al. [206] developed a plasmonic biosensor based on surface-enhanced infrared absorption that can deliver results in real time and on-site. A genetic algorithm intelligent program was employed to facilitate automation of the design process with optimal sensing performance. Most diagnostic tools need advanced laboratory instrument to read the result which prevent many portable sensors from becoming true POC devices. To solve this, Moitra et al. [207] developed a colorimetric assay with AuNPs with which the result can be observed by naked eye without the need for any laboratory signal reading system.

6.2. Machine learning

Despite of the advances in development of nanostructures for various detection purposes, the design of plasmonic sensors remain an iterative process and calls for experience from researchers. Traditional design strategy starts from computational modeling of plasmonic nanoparticles to predict their optical properties. However, these modeling tools to solve EM equations are typically time consuming. More importantly, there's no way for the forward simulations to solve the inverse problem, that is to find the required nanostructure for the target optical property. Thanks to the fast development of artificial intelligence algorithm during recent years, there exist new chances in efficient design of plasmonic nanostructures.

Machine-learning based method serves as a fast and predictive tool to model the optical properties of nanoparticles. Traditional modeling methods do the prediction via numerically solving the Maxwell equation, whose predicting results are usually limited by the resolution and observational error. Differently, neural network (NN) can discover the intrinsic correlation between the nanostructure and their optical properties from a real dataset, even though their underlying physics are unknown. As a result, NN can provide more accurate predictions than conventional modeling methods. Besides, once a neural network is trained well, it can predict the optical properties of numerous designs within a few seconds [208–210]. NN is also able to solve the inverse design problems by directly providing the required design parameters for target sensing properties [211,212]. Once a NN is trained well from the provided dataset, the mapping from design parameters to their resulting optical characteristics are established. The advanced NN tools can automatically optimizing the design parameters to achieve the target optical properties, therefore automating the entire design process. In addition to the plasmonic design, machine-learning algorithms also facilitate the characterization of plasmonic sensing. Conventional neural network (CNN) has the outstanding capability to recognize and extract the features in images, thus becoming a powerful tool in image classification. In recent years, CNN has been extensively employed in various plasmonic image analysis, including the colorimetric detection [213] and SERS detection [214,215].

6.3. Miniaturization

The main challenges in optical biosensors are the light source and the optical readout equipment. Conventional optical biosensors have taken advantage of two “equipment” from nature, the broadband daylight as the light source and the human eyes as the photodetector in the visible wavelength. One example of such a sensor is the colorimetric pregnancy test strip, in which the LSPR by the aggregated gold nanoparticles induces significant light absorption change that can be detected by human eyes. However, moving forward, improving the sensitivity and resolution of optical biosensors requires better controlled light sources and more accurate photodetectors. In recent years, thanks to the fast-growing semiconductor technologies, cellphones are packed with more and more powerful computing power and advanced cameras. This brings a unique opportunity in tackling the aforementioned challenges in the POC optical biosensors. The light emitted diode (LED) on the cell phone can act as a light source with well-controlled wavelength and intensity while the high-resolution camera can act as a sensitive photodetector for the sensing. Furthermore, the computing power on the cell phone enables the acquired optical signal to be analyzed with a complex algorithm and provides real-time diagnosis results.

6.4. Gold standard

Compared to the gold standard methods, such as diagnostics for HIV/HBV by enzyme immunoassay, detection for Dengue, Malaria and COVID-19 by PCR, and judgement for TB by growth of colony-forming units of mycobacterium tuberculosis on culture of sputum [216,217], the POC testing enabled by plasmonic nanosensors has shown high sensitivity, low cost, easy operation, and good correlation to those gold standards [218]. There is growing consensus that these screening tools can play important role in disease or biomarker detection along with existing clinical settings, instead of being used as independent technologies. For instance, reverse transcriptase PCR (RT-PCR) is currently considered to be the gold standard for the early detection of COVID-19 pioneered by the U.S. Centers for Disease Control and Prevention [219]. However, the clinical manifestation of COVID-19 can be significantly divergent from individual to individual, some patients are even asymptomatic. Therefore, physicians need to choose suitable techniques, such as chest computed tomography (CT), ELISA and lateral flow immunoassay for COVID-19 early diagnosis and clinical management [220]. RT-PCR offers the most sensitive detection, but this test takes several hours to complete and requires extensive human labor and consumable materials. Plasmonic nanosensors can reduce the time-to-result down to less than 15 minutes with high portability, although their limit of detection is still not competitive against the gold standard test. We believe rapid point-of-care technologies enabled by plasmonic nanosensors are still in development and validation, and they can serve as an alternative detection procedure for the screening of infectious diseases soon.

7. Conclusion

Advancement of nanomaterials facilitate the progress in medicine ranging from implantable biomedical devices [221–226] to disease biosensors as illustrated in this review. The recent progress on the design of plasmonic nanomaterial-based biosensors for biomarker detection with a perspective of POC applications was systematically and comprehensively reviewed. Cutting-edge works in the field focusing on the technology's design, including especially nanomaterials development, structure assembly, and target applications are examined. Although many technologies are still in the laboratory research and development phase, some of them already have met the basic requirements to become a POC device, while others have shown promising potential to become one. Challenges, however, remain in plasmonic biosensors for biomarker detection, such as using the technology for rapid and accurate testing of SARS-Cov-2 and further enhancing the sensor's accuracy and limit of detection. Still, the future of the POC plasmonic biosensing technology is full of opportunities such as miniaturization of both the sensor and the read-out machines and incorporation of machine learning.

Author contributions

C. J., Z. W. and J. M. contributed equally to the writing of significant parts of this article. J. Z. and Y. R. each wrote individual sections. C. J. compiled and edited the work. C. J. and J. X.J. Z reviewed and edited the paper. J. X.J. Z conceived the topic and supervised the work.

Declaration of competing interest

The authors declare that they have no known competing financial interests or personal relationships that could have appeared to influence the work reported in this paper.

Acknowledgment

This work was sponsored by the NIH Director's Transformative Research Award (R01HL137157) and NSF grants (ECCS 1128677, 1309686, and 1509369).

References

[1] C. Liang, J. Luan, Z. Wang, Q. Jiang, R. Gupta, S. Cao, K.-K. Liu, J.J. Morrissey, E.D. Kharasch, R.R. Naik, S. Singamaneni, Gold nanorod size-dependent fluorescence enhancement for ultrasensitive fluoroimmunoassays, ACS Appl. Mater. Interfaces 13 (2021) 11414–11423, https://doi.org/10.1021/acsami.0c20303.

[2] J. Luan, J.J. Morrissey, Z. Wang, H.G. Derami, K.K. Liu, S. Cao, Q. Jiang, C. Wang, E.D. Kharasch, R.R. Naik, S. Singamaneni, Add-on plasmonic patch as a universal fluorescence enhancer, Light Sci. Appl. 7 (2018) 2047–7538, https://doi.org/10.1038/s41377-018-0027-8.

[3] L. Scarabelli, L.M. Liz-Marzán, An extended protocol for the synthesis of monodisperse gold nanotriangles, ACS Nano (2021) 1c10538, https://doi.org/10.1021/acsnano.1c10538, acsnano.

[4] J. Luan, A. Seth, R. Gupta, Z. Wang, P. Rathi, S. Cao, H. Gholami Derami, R. Tang, B. Xu, S. Achilefu, J.J. Morrissey, S. Singamaneni, Ultrabright fluorescent nanoscale labels for the femtomolar detection of analytes with standard bioassays, Nat. Biomed. Eng. 4 (2020) 518–530, https://doi.org/10.1038/s41551-020-0547-4.

[5] M.L. Personick, M.R. Langille, J. Wu, C.A. Mirkin, Synthesis of gold hexagonal bipyramids directed by planar-twinned silver triangular nanoprisms, J. Am. Chem. Soc. 135 (2013) 3800–3803, https://doi.org/10.1021/ja400794q.

[6] H. Yoo, M.H. Jang, Size-controlled synthesis of gold bipyramids using an aqueous mixture of CTAC and salicylate anions as the soft template, Nanoscale 5 (2013) 6708, https://doi.org/10.1039/c3nr01553j.

[7] Y.-C. Yeh, B. Creran, V.M. Rotello, Gold nanoparticles: preparation, properties, and applications in bionanotechnology, Nanoscale 4 (2012) 1871–1880, https://doi.org/10.1039/c1nr11188d.

[8] J. Piella, N.G. Bastús, V. Puntes, Size-controlled synthesis of sub-10-nanometer citrate-stabilized gold nanoparticles and related optical properties, Chem. Mater. 28 (2016) 1066–1075, https://doi.org/10.1021/acs.chemmater.5b04406.

[9] A. Tadimety, Z. Wu, J.H. Molinski, R. Beckerman, C. Jin, L. Zhang, T.J. Palinski, J.X.J. Zhang, Shape effects of plasmonic gold nanoparticles for circulating tumor DNA screening, in: Proceedings of IEEE Sensors, 2020, pp. 16–19, https://doi.org/10.1109/SENSORS47125.2020.9278614.

[10] M.R. Gartia, A. Hsiao, A. Pokhriyal, S. Seo, G. Kulsharova, B.T. Cunningham, T.C. Bond, G.L. Liu, Colorimetric plasmon resonance imaging using nano Lycurgus cup arrays, Adv. Opt. Mater. 1 (2013) 68–76, https://doi.org/10.1002/adom.201200040.

[11] P. Gupta, J. Luan, Z. Wang, S. Cao, S.H. Bae, R.R. Naik, S. Singamaneni, On-demand electromagnetic hotspot generation in surface-enhanced Raman scattering substrates via "add-on" plasmonic patch, ACS Appl. Mater. Interfaces 11 (2019) 37939–37946, https://doi.org/10.1021/acsami.9b12402.

[12] L. Tang, J. Li, Plasmon-based colorimetric nanosensors for ultrasensitive molecular diagnostics, ACS Sens. 2 (2017) 857–875, https://doi.org/10.1021/acssensors.7b00282.

[13] Z. Li, L. Leustean, F. Inci, M. Zheng, U. Demirci, S. Wang, Plasmonic-based platforms for diagnosis of infectious diseases at the point-of-care, Biotechnol. Adv. 37 (2019) 107440, https://doi.org/10.1016/j.biotechadv.2019.107440.

[14] A. Tadimety, Z. Wu, J.H. Molinski, R. Beckerman, C. Jin, L. Zhang, T.J. Palinski, J.X.J. Zhang, Rational design of on-chip gold plasmonic nanoparticles towards ctDNA screening, Sci. Rep. 11 (2021), https://doi.org/10.1038/s41598-021-93207-7.

[15] D. Mabey, R.W. Peeling, A. Ustianowski, M.D. Perkins, Diagnostics for the developing world, Nat. Rev. Microbiol. 2 (2004) 231–240, https://doi.org/10.1038/nrmicro841.

[16] Z. Li, L. Leustean, F. Inci, M. Zheng, U. Demirci, S. Wang, Plasmonic-based platforms for diagnosis of infectious diseases at the point-of-care, Biotechnol. Adv. 37 (2019) 107440, https://doi.org/10.1016/j.biotechadv.2019.107440.

[17] O. Tokel, F. Inci, U. Demirci, Advances in plasmonic technologies for point of care applications, Chem. Rev. 114 (2014) 5728–5752, https://doi.org/10.1021/cr4000623.

[18] T. Mahmoudi, M. de la Guardia, B. Baradaran, Lateral flow assays towards point-of-care cancer detection: a review of current progress and future trends, Trac. Trends Anal. Chem. 125 (2020) 115842, https://doi.org/10.1016/j.trac.2020.115842.

[19] A. Prasad, J. Choi, Z. Jia, S. Park, M.R. Gartia, Nanohole array plasmonic biosensors: emerging point-of-care applications, Biosens. Bioelectron. 130 (2019) 185–203, https://doi.org/10.1016/j.bios.2019.01.037.

[20] Y. Wang, J. Zhou, J. Li, Construction of plasmonic nano-biosensor-based devices for point-of-care testing, Small Methods 1 (2017) 1–13, https://doi.org/10.1002/smtd.201700197.

[21] S.D. Bindesri, D.S. Alhatab, C.L. Brosseau, Development of an electrochemical surface-enhanced Raman spectroscopy (EC-SERS) fabric-based plasmonic sensor for point-of-care diagnostics, Analyst 143 (2018) 4128–4135, https://doi.org/10.1039/c8an01117f.

[22] D.K. Gramotnev, S.I. Bozhevolnyi, Plasmonics beyond the diffraction limit, Nat. Photonics 4 (2010) 83–91, https://doi.org/10.1038/nphoton.2009.282.

[23] M. Zhang, C. Jin, Y. Nie, Y. Ren, N. Hao, Z. Xu, L. Dong, J.X.J. Zhang, Silver nanoparticle on zinc oxide array for label-free detection of opioids through surface-enhanced Raman spectroscopy, RSC Adv. 11 (2021) 11329–11337, https://doi.org/10.1039/d1ra00760b.

[24] N. Hao, Z. Xu, Y. Nie, C. Jin, A.B. Closson, M. Zhang, J.X.J. Zhang, Microfluidics-enabled rational design of ZnO micro-/nanoparticles with enhanced photocatalysis, cytotoxicity, and piezoelectric properties, Chem. Eng. J. 378 (2019) 122222, https://doi.org/10.1016/j.cej.2019.122222.

[25] N. Hao, Y. Nie, Z. Xu, C. Jin, T.J. Fyda, J.X.J. Zhang, Microfluidics-enabled acceleration of Fenton oxidation for degradation of organic dyes with rod-like zero-valent iron nanoassemblies, J. Colloid Interface Sci. 559 (2020) 254–262, https://doi.org/10.1016/j.jcis.2019.10.042.

[26] Y. Nie, C. Jin, J.X.J. Zhang, Microfluidic in situ patterning of silver nanoparticles for surface-enhanced Raman spectroscopic sensing of biomolecules, ACS Sens. 6 (2021) 2584–2592, https://doi.org/10.1021/acssensors.1c00117.

[27] J. Zeng, Y. Zhang, T. Zeng, R. Aleisa, Z. Qiu, Y. Chen, J. Huang, D. Wang, Z. Yan, Y. Yin, Anisotropic plasmonic nanostructures for colorimetric sensing, Nano Today 32 (2020) 100855, https://doi.org/10.1016/j.nantod.2020.100855.

[28] A. Sousa-Castillo, M. Comesaña-Hermo, B. Rodríguez-González, M. Pérez-Lorenzo, Z. Wang, X.-T. Kong, A.O. Govorov, M.A. Correa-Duarte, Boosting hot electron-driven photocatalysis through anisotropic plasmonic nanoparticles with hot spots in Au–TiO 2 nanoarchitectures, J. Phys. Chem. C 120 (2016) 11690–11699, https://doi.org/10.1021/acs.jpcc.6b02370.

[29] C.S. Kumarasinghe, M. Premaratne, Q. Bao, G.P. Agrawal, Theoretical analysis of hot electron dynamics in nanorods, Sci. Rep. 5 (2015) 12140, https://doi.org/10.1038/srep12140.

[30] Z. Zhang, H. Wang, Z. Chen, X. Wang, J. Choo, L. Chen, Plasmonic colorimetric sensors based on etching and growth of noble metal nanoparticles: strategies and applications, Biosens. Bioelectron. 114 (2018) 52–65, https://doi.org/10.1016/J.BIOS.2018.05.015.

[31] S. Xu, L. Jiang, Y. Liu, P. Liu, W. Wang, X. Luo, A morphology-based ultrasensitive multicolor colorimetric assay for detection of blood glucose by enzymatic etching of plasmonic gold nanobipyramids, Anal. Chim. Acta 1071 (2019) 53–58, https://doi.org/10.1016/J.ACA.2019.04.053.

[32] A. Kinkhabwala, Z. Yu, S. Fan, Y. Avlasevich, K. Müllen, W.E. Moerner, Large single-molecule fluorescence enhancements produced by a bowtie nanoantenna, Nat. Photonics 3 (2009) 654–657, https://doi.org/10.1038/nphoton.2009.187.

[33] K. Liang, F. Liu, J. Fan, D. Sun, C. Liu, C.J. Lyon, D.W. Bernard, Y. Li, K. Yokoi, M.H. Katz, E.J. Koay, Z. Zhao, Y. Hu, Nanoplasmonic quantification of tumour-derived extracellular vesicles in plasma microsamples for diagnosis and treatment

monitoring, Nat. Biomed. Eng. 1 (2017), 0021, https://doi.org/10.1038/s41551-016-0021.
[34] T. Pinheiro, A.C. Marques, P. Carvalho, R. Martins, E. Fortunato, Paper microfluidics and tailored gold nanoparticles for nonenzymatic, colorimetric multiplex biomarker detection, ACS Appl. Mater. Interfaces 13 (2021) 3576–3590, https://doi.org/10.1021/ACSAMI.0C19089.
[35] F. Wang, N. Na, J. Ouyang, A catalytic—regulated gold nanorods etching process as a receptor with multiple readouts for protein detection, Sensor. Actuator. B Chem. 318 (2020), https://doi.org/10.1016/j.snb.2020.128215.
[36] A. Ameen, L.P. Hackett, S. Seo, F.K. Dar, M.R. Gartia, L.L. Goddard, G.L. Liu, Plasmonic sensing of oncoproteins without resonance shift using 3D periodic nanocavity in nanocup arrays, Adv. Opt. Mater. 5 (2017) 1601051, https://doi.org/10.1002/adom.201601051.
[37] A. Ameen, M.R. Gartia, A. Hsiao, T.-W. Chang, Z. Xu, G.L. Liu, Ultra-sensitive colorimetric plasmonic sensing and microfluidics for biofluid diagnostics using nanohole array, J. Nanomater. (2015) 1–21, https://doi.org/10.1155/2015/460895, 2015.
[38] T.-W. Chang, X. Wang, A. Hsiao, Z. Xu, G. Lin, R. Gartia, X. Liu, L. Liu, Bifunctional Nano Lycurgus Cup Array Plasmonic Sensor for Colorimetric Sensing and Surface-Enhanced Raman Spectroscopy, 2015, https://doi.org/10.1002/adom.201500092.
[39] E. Balaur, S. O' Toole, A.J. Spurling, G.B. Mann, B. Yeo, K. Harvey, C. Sadatnajafi, E. Hanssen, J. Orian, K.A. Nugent, B.S. Parker, B. Abbey, Colorimetric histology using plasmonically active microscope slides, Nature 598 (2021) 65–71, https://doi.org/10.1038/s41586-021-03835-2.
[40] S.K. Misra, K. Dighe, A.S. Schwartz-Duval, Z. Shang, L.T. Labriola, D. Pan, In situ plasmonic generation in functional ionic-gold-nanogel scaffold for rapid quantitative bio-sensing, Biosens. Bioelectron. 120 (2018) 77–84, https://doi.org/10.1016/j.bios.2018.08.019.
[41] S.K. Vashist, E. Marion Schneider, R. Zengerle, F. von Stetten, J.H.T. Luong, Graphene-based rapid and highly-sensitive immunoassay for C-reactive protein using a smartphone-based colorimetric reader, Biosens. Bioelectron. 66 (2015) 169–176, https://doi.org/10.1016/j.bios.2014.11.017.
[42] O. Hosu, A. Ravalli, G.M. lo Piccolo, C. Cristea, R. Sandulescu, G. Marrazza, Smartphone-based immunosensor for CA125 detection, Talanta 166 (2017) 234–240, https://doi.org/10.1016/j.talanta.2017.01.073.
[43] L. Zheng, P. Qi, D. Zhang, A simple, rapid and cost-effective colorimetric assay based on the 4-mercaptophenylboronic acid functionalized silver nanoparticles for bacteria monitoring, Sensor. Actuator. B Chem. 260 (2018) 983–989, https://doi.org/10.1016/j.snb.2018.01.115.
[44] K.L. Lee, M.L. You, C.H. Tsai, E.H. Lin, S.Y. Hsieh, M.H. Ho, J.C. Hsu, P.K. Wei, Nanoplasmonic biochips for rapid label-free detection of imidacloprid pesticides with a smartphone, Biosens. Bioelectron. 75 (2016) 88–95, https://doi.org/10.1016/j.bios.2015.08.010.
[45] H. Guner, E. Ozgur, G. Kokturk, M. Celik, E. Esen, A.E. Topal, S. Ayas, Y. Uludag, C. Elbuken, A. Dana, A smartphone based surface plasmon resonance imaging (SPRi) platform for on-site biodetection, Sensor. Actuator. B Chem. 239 (2017) 571–577, https://doi.org/10.1016/j.snb.2016.08.061.
[46] W. il Lee, S. Shrivastava, L.T. Duy, B. Yeong Kim, Y.M. Son, N.E. Lee, A smartphone imaging-based label-free and dual-wavelength fluorescent biosensor with high sensitivity and accuracy, Biosens. Bioelectron. 94 (2017) 643–650, https://doi.org/10.1016/j.bios.2017.03.061.
[47] J. Bian, X. Xing, S. Zhou, Z. Man, Z. Lu, W. Zhang, Patterned plasmonic gradient for high-precision biosensing using a smartphone reader, Nanoscale 11 (2019) 12471–12476, https://doi.org/10.1039/c9nr00455f.
[48] Y. Lu, Y. Lin, Z. Zheng, X. Tang, J. Lin, X. Liu, M. Liu, G. Chen, S. Qiu, T. Zhou, Y. Lin, S. Feng, Label free hepatitis B detection based on serum derivative surface enhanced Raman spectroscopy combined with multivariate analysis, Biomed. Opt Express 9 (2018) 4755, https://doi.org/10.1364/BOE.9.004755.
[49] M.P. Peng, W. Ma, Y.T. Long, Alcohol dehydrogenase-catalyzed gold nanoparticle seed-mediated growth allows reliable detection of disease biomarkers with the naked eye, Anal. Chem. 87 (2015) 5891–5896, https://doi.org/10.1021/acs.analchem.5b00287.
[50] P. Valentini, P.P. Pompa, A universal polymerase chain reaction developer, Angew. Chem. Int. Ed. 55 (2016) 2157–2160, https://doi.org/10.1002/anie.201511010.
[51] X. Fu, Z. Cheng, J. Yu, P. Choo, L. Chen, J. Choo, A SERS-based lateral flow assay biosensor for highly sensitive detection of HIV-1 DNA, Biosens. Bioelectron. 78 (2016) 530–537, https://doi.org/10.1016/j.bios.2015.11.099.
[52] T.T. Tsai, C.Y. Huang, C.A. Chen, S.W. Shen, M.C. Wang, C.M. Cheng, C.F. Chen, Diagnosis of tuberculosis using colorimetric gold nanoparticles on a paper-based analytical device, ACS Sens. 2 (2017) 1345–1354, https://doi.org/10.1021/acssensors.7b00450.
[53] A.C. Crawford, L.B. Laurentius, T.S. Mulvihill, J.H. Granger, J.S. Spencer, D. Chatterjee, K.E. Hanson, M.D. Porter, Detection of the tuberculosis antigenic marker mannose-capped lipoarabinomannan in pretreated serum by surface-enhanced Raman scattering, Analyst 142 (2017) 186–196, https://doi.org/10.1039/C6AN02110G.
[54] A. Ahmadivand, B. Gerislioglu, Z. Ramezani, A. Kaushik, P. Manickam, S.A. Ghoreishi, Functionalized terahertz plasmonic metasensors: femtomolar-level detection of SARS-CoV-2 spike proteins, Biosens. Bioelectron. 177 (2021) 112971, https://doi.org/10.1016/j.bios.2021.112971.
[55] O. Hosu, A. Ravalli, G.M. lo Piccolo, C. Cristea, R. Sandulescu, G. Marrazza, Smartphone-based immunosensor for CA125 detection, Talanta 166 (2017) 234–240, https://doi.org/10.1016/j.talanta.2017.01.073.
[56] P. Moitra, M. Alafeef, K. Dighe, M.B. Frieman, D. Pan, Selective naked-eye detection of SARS-CoV-2 mediated by N gene targeted antisense oligonucleotide capped plasmonic nanoparticles, ACS Nano 14 (2020) 7617–7627, https://doi.org/10.1021/acsnano.0c03822.
[57] L. Zhang, J. Wang, J. Zhang, Y. Liu, L. Wu, J. Shen, Y. Zhang, Y. Hu, Q. Fan, W. Huang, L. Wang, Individual Au-nanocube based plasmonic nanoprobe for cancer relevant MicroRNA biomarker detection, ACS Sens. 2 (2017) 1435–1440, https://doi.org/10.1021/acssensors.7b00322.
[58] Y. Tian, L. Zhang, J. Shen, L. Wu, H. He, D.-L. Ma, C.-H. Leung, W. Wu, Q. Fan, W. Huang, L. Wang, An individual nanocube-based plasmonic biosensor for real-time monitoring the structural switch of the telomeric G-quadruplex, Small 12 (2016) 2913–2920, https://doi.org/10.1002/smll.201600041.
[59] J. Tang, P. Xiong, Y. Cheng, Y. Chen, S. Peng, Z.-Q. Zhu, Enzymatic oxydate-triggered AgNPs etching: a novel signal-on photoelectrochemical immunosensing platform based on Ag@AgCl nanocubes loaded RGO plasmonic heterostructure, Biosens. Bioelectron. 130 (2019) 125–131, https://doi.org/10.1016/j.bios.2019.01.014.
[60] D. Zhang, Y. Sun, Q. Wu, P. Ma, H. Zhang, Y. Wang, D. Song, Enhancing sensitivity of surface plasmon resonance biosensor by Ag nanocubes/chitosan composite for the detection of mouse IgG, Talanta 146 (2016) 364–368, https://doi.org/10.1016/j.talanta.2015.08.050.
[61] C. Zhu, X. Wang, X. Shi, F. Yang, G. Meng, Q. Xiong, Y. Ke, H. Wang, Y. Lu, N. Wu, Detection of dithiocarbamate pesticides with a spongelike surface-enhanced Raman scattering substrate made of reduced graphene oxide-wrapped silver nanocubes, ACS Appl. Mater. Interfaces 9 (2017) 39618–39625, https://doi.org/10.1021/acsami.7b13479.
[62] S. Mariani, S. Scarano, J. Spadavecchia, M. Minunni, A reusable optical biosensor for the ultrasensitive and selective detection of unamplified human genomic DNA with gold nanostars, Biosens. Bioelectron. 74 (2015) 981–988, https://doi.org/10.1016/j.bios.2015.07.071.
[63] M. Reyes, M. Piotrowski, S.K. Ang, J. Chan, S. He, J.J.H. Chu, J.C.Y. Kah, Exploiting the anti-aggregation of gold nanostars for rapid detection of hand, foot, and mouth disease causing enterovirus 71 using surface-enhanced Raman spectroscopy, Anal. Chem. 89 (2017) 5373–5381, https://doi.org/10.1021/acs.analchem.7b00066.
[64] S.R. Ahmed, É. Nagy, S. Neethirajan, Self-assembled star-shaped chiroplasmonic gold nanoparticles for an ultrasensitive chiro-immunosensor for viruses, RSC Adv. 7 (2017) 40849–40857, https://doi.org/10.1039/C7RA07175B.
[65] M. Sánchez-Purrà, M. Carré-Camps, H. de Puig, I. Bosch, L. Gehrke, K. Hamad-Schifferli, Surface-enhanced Raman spectroscopy-based sandwich immunoassays for multiplexed detection of Zika and dengue viral biomarkers, ACS Infect. Dis. 3 (2017) 767–776, https://doi.org/10.1021/acsinfecdis.7b00110.
[66] W. Wang, L. Zhang, L. Li, Y. Tian, A single nanoprobe for ratiometric imaging and biosensing of hypochlorite and glutathione in live cells using surface-enhanced Raman scattering, Anal. Chem. 88 (2016) 9518–9523, https://doi.org/10.1021/acs.analchem.6b02081.
[67] S. Park, X. Xiao, J. Min, C. Mun, H.S. Jung, V. Giannini, R. Weissleder, S.A. Maier, H. Im, D. Kim, Self-assembly of nanoparticle-spiked pillar arrays for plasmonic biosensing, Adv. Funct. Mater. 29 (2019) 1904257, https://doi.org/10.1002/adfm.201904257.
[68] W. Sun, S. Yuan, H. Huang, N. Liu, Y. Tan, A label-free biosensor based on localized surface plasmon resonance for diagnosis of tuberculosis, J. Microbiol. Methods 142 (2017) 41–45, https://doi.org/10.1016/j.mimet.2017.09.007.
[69] A. Tadimety, Y. Zhang, K.M. Kready, T.J. Palinski, G.J. Tsongalis, J.X.J. Zhang, Design of peptide nucleic acid probes on plasmonic gold nanorods for detection of circulating tumor DNA point mutations, Biosens. Bioelectron. 130 (2019) 236–244, https://doi.org/10.1016/j.bios.2019.01.045.
[70] F. Zang, Z. Su, L. Zhou, K. Konduru, G. Kaplan, S.Y. Chou, Ultrasensitive ebola virus antigen sensing via 3D nanoantenna arrays, Adv. Mater. 31 (2019) 1902331, https://doi.org/10.1002/adma.201902331.
[71] C.M. Das, Y. Guo, G. Yang, L. Kang, G. Xu, H.P. Ho, K.T. Yong, Gold nanorod assisted enhanced plasmonic detection scheme of COVID-19 SARS-CoV-2 spike protein, Adv. Theory Simul. 3 (2020) 1–8, https://doi.org/10.1002/adts.202000185.
[72] P.M. Kosaka, V. Pini, M. Calleja, J. Tamayo, Ultrasensitive detection of HIV-1 p24 antigen by a hybrid nanomechanical-optoplasmonic platform with potential for detecting HIV-1 at first week after infection, PLoS One 12 (2017), e0171899, https://doi.org/10.1371/journal.pone.0171899.
[73] J. Kim, S.Y. Oh, S. Shukla, S.B. Hong, N.S. Heo, VivekK. Bajpai, H.S. Chun, C.-H. Jo, B.G. Choi, Y.S. Huh, Y.-K. Han, Heteroassembled gold nanoparticles with sandwich-immunoassay LSPR chip format for rapid and sensitive detection of hepatitis B virus surface antigen (HBsAg), Biosens. Bioelectron. 107 (2018) 118–122, https://doi.org/10.1016/j.bios.2018.02.019.
[74] R. Funari, K.-Y. Chu, A.Q. Shen, Detection of antibodies against SARS-CoV-2 spike protein by gold nanospikes in an opto-microfluidic chip, Biosens. Bioelectron. 169 (2020) 112578, https://doi.org/10.1016/j.bios.2020.112578.
[75] F. Zou, X. Wang, F. Qi, K. Koh, J. Lee, H. Zhou, H. Chen, Magneto-plamonic nanoparticles enhanced surface plasmon resonance TB sensor based on recombinant gold binding antibody, Sensor. Actuator. B Chem. 250 (2017) 356–363, https://doi.org/10.1016/j.snb.2017.04.162.
[76] N. Fakhri, S. Abarghoei, M. Dadmehr, M. Hosseini, H. Sabahi, M.R. Ganjali, Paper based colorimetric detection of miRNA-21 using Ag/Pt nanoclusters, Spectrochim. Acta Mol. Biomol. Spectrosc. 227 (2020) 117529, https://doi.org/10.1016/j.saa.2019.117529.
[77] A. Minopoli, B. della Ventura, B. Lenyk, F. Gentile, J.A. Tanner, A. Offenhäusser, D. Mayer, R. Velotta, Ultrasensitive antibody-aptamer plasmonic biosensor for

malaria biomarker detection in whole blood, Nat. Commun. 11 (2020) 6134, https://doi.org/10.1038/s41467-020-19755-0.
[78] M.R. Gonçalves, Plasmonic nanoparticles: fabrication, simulation and experiments, J. Phys. Appl. Phys. 47 (2014), https://doi.org/10.1088/0022-3727/47/21/213001.
[79] M. Faraday, LIX, Experimental relations of gold (and other metals) to light.—The bakerian lecture , The London, Edinburgh, and Dublin, Philosoph. Magaz. J. Sci. 14 (1857) 512–539, https://doi.org/10.1080/14786445708642424.
[80] S. Yu, H. Ammari, Plasmonic interaction between nanospheres, SIAM Rev. 60 (2018) 356–385, https://doi.org/10.1137/17M1115319.
[81] J. Turkevich, P.C. Stevenson, J. Hillier, A study of the nucleation and growth processes in the synthesis of colloidal gold, Discuss. Faraday Soc. 11 (1951) 55–75, https://doi.org/10.1039/DF9511100055.
[82] M. Brust, M. Walker, D. Bethell, D.J. Schiffrin, R. Whyman, Synthesis of thiol-derivatised gold nanoparticles in a two-phase Liquid–Liquid system, J. Chem. Soc. Chem. Commun. (1994) 801–802, https://doi.org/10.1039/C39940000801.
[83] X. Fu, Z. Cheng, J. Yu, P. Choo, L. Chen, J. Choo, A SERS-based lateral flow assay biosensor for highly sensitive detection of HIV-1 DNA, Biosens. Bioelectron. 78 (2016) 530–537, https://doi.org/10.1016/j.bios.2015.11.099.
[84] P. Valentini, P.P. Pompa, A universal polymerase chain reaction developer, Angew. Chem. Int. Ed. 55 (2016) 2157–2160, https://doi.org/10.1002/anie.201511010.
[85] T.T. Tsai, C.Y. Huang, C.A. Chen, S.W. Shen, M.C. Wang, C.M. Cheng, C.F. Chen, Diagnosis of tuberculosis using colorimetric gold nanoparticles on a paper-based analytical device, ACS Sens. 2 (2017) 1345–1354, https://doi.org/10.1021/acssensors.7b00450.
[86] P. Moitra, M. Alafeef, M. Alafeef, M. Alafeef, K. Dighe, M.B. Frieman, D. Pan, D. Pan, D. Pan, Selective naked-eye detection of SARS-CoV-2 mediated by N gene targeted antisense oligonucleotide capped plasmonic nanoparticles, ACS Nano 14 (2020) 7617–7627, https://doi.org/10.1021/acsnano.0c03822.
[87] J. Kim, S.Y. Oh, S. Shukla, S.B. Hong, N.S. Heo, V.K. Bajpai, H.S. Chun, C.H. Jo, B.G. Choi, Y.S. Huh, Y.K. Han, Heteroassembled gold nanoparticles with sandwich-immunoassay LSPR chip format for rapid and sensitive detection of hepatitis B virus surface antigen (HBsAg), Biosens. Bioelectron. 107 (2018) 118–122, https://doi.org/10.1016/j.bios.2018.02.019.
[88] N.G. Bastús, J. Comenge, V. Puntes, Kinetically controlled seeded growth synthesis of citrate-stabilized gold nanoparticles of up to 200 nm: size focusing versus ostwald ripening, Langmuir 27 (2011) 11098–11105, https://doi.org/10.1021/la201938u.
[89] N. Leopold, B. Lendl, A new method for fast preparation of highly surface-enhanced Raman scattering (SERS) active silver colloids at room temperature by reduction of silver nitrate with hydroxylamine hydrochloride, J. Phys. Chem. B 107 (2003) 5723–5727, https://doi.org/10.1021/jp027460u.
[90] Y. Lu, Y. Lin, Z. Zheng, X. Tang, J. Lin, X. Liu, M. Liu, G. Chen, S. Qiu, T. Zhou, Y. Lin, S. Feng, Label free hepatitis B detection based on serum derivative surface enhanced Raman spectroscopy combined with multivariate analysis, Biomed. Opt Express 9 (2018) 4755, https://doi.org/10.1364/boe.9.004755.
[91] M.P. Peng, W. Ma, Y.T. Long, Alcohol dehydrogenase-catalyzed gold nanoparticle seed-mediated growth allows reliable detection of disease biomarkers with the naked eye, Anal. Chem. 87 (2015) 5891–5896, https://doi.org/10.1021/acs.analchem.5b00287.
[92] R. Elghanian, J.J. Storhoff, R.C. Mucic, R.L. Letsinger, C.A. Mirkin, Selective colorimetric detection of polynucleotides based on the distance-dependent optical properties of gold nanoparticles, Science 277 (1997) 1078–1081, https://doi.org/10.1126/science.277.5329.1078.
[93] A. Ahmadivand, B. Gerislioglu, Z. Ramezani, A. Kaushik, P. Manickam, S.A. Ghoreishi, Functionalized terahertz plasmonic metasensors: femtomolar-level detection of SARS-CoV-2 spike proteins, Biosens. Bioelectron. 177 (2021) 112971, https://doi.org/10.1016/j.bios.2021.112971.
[94] T. Wu, Y. Cao, Y. Zhang, Z. Zheng, J. Li, H. Li, Entropy-driven DNA amplification networks coupled with hollow porous Au–Ag nanospheres for split-type plasmonic photothermal biosensing, ACS Appl. Nano Mater. 5 (2022) 537–545, https://doi.org/10.1021/acsanm.1c03365.
[95] Y. Jiang, M. Shi, Y. Liu, S. Wan, C. Cui, L. Zhang, W. Tan, Aptamer/AuNP biosensor for colorimetric profiling of exosomal proteins, Angew. Chem. 129 (2017) 12078–12082, https://doi.org/10.1002/ange.201703807.
[96] S. Rostami, A. Mehdinia, R. Niroumand, A. Jabbari, Enhanced LSPR performance of graphene nanoribbons-silver nanoparticles hybrid as a colorimetric sensor for sequential detection of dopamine and glutathione, Anal. Chim. Acta 1120 (2020) 11–23, https://doi.org/10.1016/j.aca.2020.04.060.
[97] D. Han, Y. Yan, X. Bian, J. Wang, M. Zhao, X. Duan, L. Kong, W. Cheng, S. Ding, A novel electrochemical biosensor based on peptidoglycan and platinum-nickel-copper nano-cube for rapid detection of Gram-positive bacteria, Microchim. Acta 187 (2020) 607, https://doi.org/10.1007/s00604-020-04581-4.
[98] H. bin Jeon, P.V. Tsalu, J.W. Ha, Shape effect on the refractive index sensitivity at localized surface plasmon resonance inflection points of single gold nanocubes with vertices, Sci. Rep. 9 (2019) 13635, https://doi.org/10.1038/s41598-019-50032-3.
[99] J.-S. Ye, C.-W. Chen, C.-L. Lee, Pd nanocube as non-enzymatic glucose sensor, Sensor. Actuator. B Chem. 208 (2015) 569–574, https://doi.org/10.1016/j.snb.2014.11.091.
[100] P. Yang, L. Wang, Q. Wu, Z. Chen, X. Lin, A method for determination of glucose by an amperometric bienzyme biosensor based on silver nanocubes modified Au electrode, Sensor. Actuator. B Chem. 194 (2014) 71–78, https://doi.org/10.1016/j.snb.2013.12.074.
[101] J.C. Claussen, A.D. Franklin, A. ul Haque, D.M. Porterfield, T.S. Fisher, Electrochemical biosensor of nanocube-augmented carbon nanotube networks, ACS Nano 3 (2009) 37–44, https://doi.org/10.1021/nn800682m.
[102] J. Ren, W. Shi, K. Li, Z. Ma, Ultrasensitive platinum nanocubes enhanced amperometric glucose biosensor based on chitosan and nafion film, Sensor. Actuator. B Chem. 163 (2012) 115–120, https://doi.org/10.1016/j.snb.2012.01.017.
[103] J. Yang, W.-D. Zhang, S. Gunasekaran, An amperometric non-enzymatic glucose sensor by electrodepositing copper nanocubes onto vertically well-aligned multi-walled carbon nanotube arrays, Biosens. Bioelectron. 26 (2010) 279–284, https://doi.org/10.1016/j.bios.2010.06.014.
[104] A.W. Powell, D.M. Coles, R.A. Taylor, A.A.R. Watt, H.E. Assender, J.M. Smith, Plasmonic gas sensing using nanocube patch antennas, Adv. Opt. Mater. 4 (2016) 634–642, https://doi.org/10.1002/adom.201500602.
[105] C. Noguez, Surface plasmons on metal nanoparticles: the influence of shape and physical environment, J. Phys. Chem. C 111 (2007) 3806–3819, https://doi.org/10.1021/jp066539m.
[106] S.E. Skrabalak, L. Au, X. Li, Y. Xia, Facile synthesis of Ag nanocubes and Au nanocages, Nat. Protoc. 2 (2007) 2182–2190, https://doi.org/10.1038/nprot.2007.326.
[107] A.R. Siekkinen, J.M. McLellan, J. Chen, Y. Xia, Rapid synthesis of small silver nanocubes by mediating polyol reduction with a trace amount of sodium sulfide or sodium hydrosulfide, Chem. Phys. Lett. 432 (2006) 491–496, https://doi.org/10.1016/j.cplett.2006.10.095.
[108] Y. Sun, Y. Xia, Shape-controlled synthesis of gold and silver nanoparticles, ChemInform 34 (2003) 2176–2180, https://doi.org/10.1002/chin.200310226.
[109] L. Zhang, J. Wang, J. Zhang, Y. Liu, L. Wu, J. Shen, Y. Zhang, Y. Hu, Q. Fan, W. Huang, L. Wang, Individual Au-nanocube based plasmonic nanoprobe for cancer relevant MicroRNA biomarker detection, ACS Sens. 2 (2017) 1435–1440, https://doi.org/10.1021/acssensors.7b00322.
[110] M. Kim, S.M. Ko, C. Lee, J. Son, J. Kim, J.M. Kim, J.M. Nam, Hierarchic interfacial nanocube assembly for sensitive, selective, and quantitative DNA detection with surface-enhanced Raman scattering, Anal. Chem. 91 (2019) 10467–10476, https://doi.org/10.1021/acs.analchem.9b01272.
[111] J. Li, J. Wang, Y.S. Grewal, C.B. Howard, L.J. Raftery, S. Mahler, Y. Wang, M. Trau, Multiplexed SERS detection of soluble cancer protein biomarkers with gold-silver alloy nanoboxes and nanoyeast single-chain variable fragments, Anal. Chem. 90 (2018) 10377–10384, https://doi.org/10.1021/acs.analchem.8b02216.
[112] K.-X. Xie, L.-T. Xu, Y.-Y. Zhai, Z.-C. Wang, M. Chen, X.-H. Pan, S.-H. Cao, Y.-Q. Li, The synergistic enhancement of silver nanocubes and graphene oxide on surface plasmon-coupled emission, Talanta 195 (2019) 752–756, https://doi.org/10.1016/j.talanta.2018.11.112.
[113] O.J. Achadu, F. Abe, T. Suzuki, E.Y. Park, Molybdenum trioxide nanocubes aligned on a graphene oxide substrate for the detection of norovirus by surface-enhanced Raman scattering, ACS Appl. Mater. Interfaces 12 (2020) 43522–43534, https://doi.org/10.1021/acsami.0c14729.
[114] O.J. Achadu, F. Abe, F. Hossain, F. Nasrin, M. Yamazaki, T. Suzuki, E.Y. Park, Sulfur-doped carbon dots@polydopamine-functionalized magnetic silver nanocubes for dual-modality detection of norovirus, Biosens. Bioelectron. 193 (2021), https://doi.org/10.1016/j.bios.2021.113540.
[115] Y. Liu, N. Lyu, V.K. Rajendran, J. Piper, A. Rodger, Y. Wang, Sensitive and direct DNA mutation detection by surface-enhanced Raman spectroscopy using rational designed and tunable plasmonic nanostructures, Anal. Chem. 92 (2020) 5708–5716, https://doi.org/10.1021/acs.analchem.9b04183.
[116] S. Chatterjee, A.B. Ringane, A. Arya, G.M. Das, V.R. Dantham, R. Laha, S. Hussian, A high-yield, one-step synthesis of surfactant-free gold nanostars and numerical study for single-molecule SERS application, J. Nanoparticle Res. 18 (2016) 242, https://doi.org/10.1007/s11051-016-3557-0.
[117] T. Lee, G.H. Kim, S.M. Kim, K. Hong, Y. Kim, C. Park, H. Sohn, J. Min, Label-free localized surface plasmon resonance biosensor composed of multi-functional DNA 3 way junction on hollow Au spike-like nanoparticles (HAuSN) for avian influenza virus detection, Colloids Surf. B Biointerfaces 182 (2019), https://doi.org/10.1016/j.colsurfb.2019.06.070.
[118] Y.H. Ngo, D. Li, G.P. Simon, G. Garnier, Gold nanoparticle-paper as a three-dimensional surface enhanced Raman scattering substrate, Langmuir 28 (2012) 8782–8790, https://doi.org/10.1021/la3012734.
[119] P.M. Mendes, S. Jacke, K. Critchley, J. Plaza, Y. Chen, K. Nikitin, R.E. Palmer, J.A. Preece, S.D. Evans, D. Fitzmaurice, Gold nanoparticle patterning of silicon wafers using chemical e-beam lithography, Langmuir 20 (2004) 3766–3768, https://doi.org/10.1021/la049803g.
[120] M.K. Corbierre, J. Beerens, R.B. Lennox, Gold nanoparticles generated by electron beam lithography of gold(I)-thiolate thin films, Chem. Mater. 17 (2005) 5774–5779, https://doi.org/10.1021/cm051085b.
[121] M. Kolíbal, M. Konečný, F. Ligmajer, D. Škoda, T. Vystavěl, J. Zlámal, P. Varga, T. Šikola, Guided assembly of gold colloidal nanoparticles on silicon substrates prepatterned by charged particle beams, ACS Nano 6 (2012) 10098–10106, https://doi.org/10.1021/nn3038226.
[122] J. Spadavecchia, P. Prete, N. Lovergine, L. Tapfer, R. Rella, Au nanoparticles prepared by physical method on Si and sapphire substrates for biosensor applications, J. Phys. Chem. B 109 (2005) 17347–17349, https://doi.org/10.1021/jp053194j.
[123] O. Bibikova, J. Haas, A.I. López-Lorente, A. Popov, M. Kinnunen, I. Meglinski, B. Mizaikoff, Towards enhanced optical sensor performance: SEIRA and SERS with plasmonic nanostars, Analyst 142 (2017) 951–958, https://doi.org/10.1039/c6an02596j.

[124] J. Shen, Y. Li, H. Gu, F. Xia, X. Zuo, Recent development of sandwich assay based on the nanobiotechnologies for proteins, nucleic acids, small molecules, and ions, Chem. Rev. 114 (2014) 7631–7677, https://doi.org/10.1021/cr300248x.
[125] X. Pei, B. Zhang, J. Tang, B. Liu, W. Lai, D. Tang, Sandwich-type immunosensors and immunoassays exploiting nanostructure labels: a review, Anal. Chim. Acta 758 (2013) 1–18, https://doi.org/10.1016/j.aca.2012.10.060.
[126] J. Kim, S.Y. Oh, S. Shukla, S.B. Hong, N.S. Heo, V.K. Bajpai, H.S. Chun, C.H. Jo, B.G. Choi, Y.S. Huh, Y.K. Han, Heteroassembled gold nanoparticles with sandwich-immunoassay LSPR chip format for rapid and sensitive detection of hepatitis B virus surface antigen (HBsAg), Biosens. Bioelectron. 107 (2018) 118–122, https://doi.org/10.1016/j.bios.2018.02.019.
[127] A.C. Crawford, L.B. Laurentius, T.S. Mulvihill, J.H. Granger, J.S. Spencer, D. Chatterjee, K.E. Hanson, M.D. Porter, Detection of the tuberculosis antigenic marker mannose-capped lipoarabinomannan in pretreated serum by surface-enhanced Raman scattering, Analyst 142 (2017) 186–196, https://doi.org/10.1039/c6an02110g.
[128] C.M. Das, Y. Guo, G. Yang, L. Kang, G. Xu, H.P. Ho, K.T. Yong, Gold Nanorod Assisted Enhanced Plasmonic Detection Scheme of COVID-19 SARS-CoV-2 Spike Protein, Advanced Theory and Simulations, vol. 3, 2020, https://doi.org/10.1002/adts.202000185.
[129] W. Lee, S.M. Shaban, D.G. Pyun, D.H. Kim, Solid-phase colorimetric apta-biosensor for thrombin detection, Thin Solid Films (2019) 686, https://doi.org/10.1016/j.tsf.2019.137428.
[130] F. Zou, X. Wang, F. Qi, K. Koh, J. Lee, H. Zhou, H. Chen, Magneto-plamonic nanoparticles enhanced surface plasmon resonance TB sensor based on recombinant gold binding antibody, Sensor. Actuator. B Chem. 250 (2017) 356–363, https://doi.org/10.1016/j.snb.2017.04.162.
[131] B. Zhang, R.B. Kumar, H. Dai, B.J. Feldman, A plasmonic chip for biomarker discovery and diagnosis of type 1 diabetes, Nat. Med. 20 (2014) 948–953, https://doi.org/10.1038/nm.3619.
[132] X. Li, T. Kuznetsova, N. Cauwenberghs, M. Wheeler, H. Maecker, J.C. Wu, F. Haddad, H. Dai, Autoantibody profiling on a plasmonic nano-gold chip for the early detection of hypertensive, Proc. Natl. Acad. Sci. U. S. A 114 (2017) 7089–7094, https://doi.org/10.1073/pnas.1621457114.
[133] J.R. Mejía-Salazar, O.N. Oliveira, Plasmon. Biosens. Chem. Rev. 118 (2018) 10617–10625, https://doi.org/10.1021/acs.chemrev.8b00359.
[134] B. Špačková, P. Wrobel, M. Bocková, J. Homola, Optical biosensors based on plasmonic nanostructures: a review, Proc. IEEE 104 (2016) 2380–2408, https://doi.org/10.1109/JPROC.2016.2624340.
[135] A. Mühlig, T. Bocklitz, I. Labugger, S. Dees, S. Henk, E. Richter, S. Andres, M. Merker, S. Stöckel, K. Weber, D. Cialla-May, J. Popp, LOC-SERS: a promising closed system for the identification of mycobacteria, Anal. Chem. 88 (2016) 7998–8004, https://doi.org/10.1021/acs.analchem.6b01152.
[136] L.W. Yap, H. Chen, Y. Gao, K. Petkovic, Y. Liang, K.J. Si, H. Wang, Z. Tang, Y. Zhu, W. Cheng, Bifunctional plasmonic-magnetic particles for an enhanced microfluidic SERS immunoassay, Nanoscale 9 (2017) 7822–7829, https://doi.org/10.1039/c7nr01511a.
[137] J. Zhou, F. Tao, J. Zhu, S. Lin, Z. Wang, X. Wang, J.Y. Ou, Y. Li, Q.H. Liu, Portable tumor biosensing of serum by plasmonic biochips in combination with nanoimprint and microfluidics, Nanophotonics 8 (2019) 307–316, https://doi.org/10.1515/nanoph-2018-0173.
[138] A. Vázquez-Guardado, S. Barkam, M. Peppler, A. Biswas, W. Dennis, S. Das, S. Seal, D. Chanda, Enzyme-free plasmonic biosensor for direct detection of neurotransmitter dopamine from whole blood, Nano Lett. 19 (2019) 449–454, https://doi.org/10.1021/acs.nanolett.8b04253.
[139] F. Inci, Y. Saylan, A.M. Kojouri, M.G. Ogut, A. Denizli, U. Demirci, A disposable microfluidic-integrated hand-held plasmonic platform for protein detection, Appl. Mater. Today 18 (2020), https://doi.org/10.1016/j.apmt.2019.100478.
[140] Z. Geng, Q. Kan, J. Yuan, H. Chen, A route to low-cost nanoplasmonic biosensor integrated with optofluidic-portable platform, Sensor. Actuator. B Chem. 195 (2014) 682–691, https://doi.org/10.1016/j.snb.2014.01.110.
[141] M. Soler, A. Belushkin, A. Cavallini, C. Kebbi-Beghdadi, G. Greub, H. Altug, Multiplexed nanoplasmonic biosensor for one-step simultaneous detection of Chlamydia trachomatis and Neisseria gonorrhoeae in urine, Biosens. Bioelectron. 94 (2017) 560–567, https://doi.org/10.1016/j.bios.2017.03.047.
[142] E.C. Peláez, M.C. Estevez, A. Mongui, M.C. Menéndez, C. Toro, O.L. Herrera-Sandoval, J. Robledo, M.J. García, P. del Portillo, L.M. Lechuga, Detection and quantification of HspX antigen in sputum samples using plasmonic biosensing: toward a real point-of-care (POC) for tuberculosis diagnosis, ACS Infect. Dis. 6 (2020) 1110–1120, https://doi.org/10.1021/acsinfecdis.9b00502.
[143] R. Funari, K.Y. Chu, A.Q. Shen, Detection of antibodies against SARS-CoV-2 spike protein by gold nanospikes in an opto-microfluidic chip, Biosens. Bioelectron. 169 (2020), https://doi.org/10.1016/j.bios.2020.112578.
[144] A.W. Martinez, S.T. Phillips, M.J. Butte, G.M. Whitesides, Patterned paper as a platform for inexpensive, low-volume, portable bioassays, Angew. Chem. 119 (2007) 1340–1342, https://doi.org/10.1002/ange.200603817.
[145] E. Carrilho, A.W. Martinez, G.M. Whitesides, Understanding wax printing: a simple micropatterning process for paper-based microfluidics, Anal. Chem. 81 (2009) 7091–7095, https://doi.org/10.1021/ac901071p.
[146] K. Abe, K. Kotera, K. Suzuki, D. Citterio, Inkjet-printed paperfluidic immuno-chemical sensing device, Anal. Bioanal. Chem. 398 (2010) 885–893, https://doi.org/10.1007/s00216-010-4011-2.
[147] A. Savolainen, Y. Zhang, D. Rochefort, U. Holopainen, T. Erho, J. Virtanen, M. Smolander, Printing of polymer microcapsules for enzyme immobilization on paper substrate, Biomacromolecules 12 (2011), https://doi.org/10.1021/bm2003434, 2008–2015.
[148] L. Ouyang, C. Wang, F. Du, T. Zheng, H. Liang, Electrochromatographic separations of multi-component metal complexes on a microfluidic paper-based device with a simplified photolithography, RSC Adv. 4 (2014) 1093–1101, https://doi.org/10.1039/c3ra43625j.
[149] C.L. Sones, I.N. Katis, P.J.W. He, B. Mills, M.F. Namiq, P. Shardlow, M. Ibsen, R.W. Eason, Laser-induced photo-polymerisation for creation of paper-based fluidic devices, Lab Chip 14 (2014) 4567–4574, https://doi.org/10.1039/c4lc00850b.
[150] N. Fakhri, S. Abarghoei, M. Dadmehr, M. Hosseini, H. Sabahi, M.R. Ganjali, Paper based colorimetric detection of miRNA-21 using Ag/Pt nanoclusters, Spectrochim. Acta Mol. Biomol. Spectrosc. 227 (2020), https://doi.org/10.1016/j.saa.2019.117529.
[151] M. Srisa-Art, K.E. Boehle, B.J. Geiss, C.S. Henry, Highly sensitive detection of Salmonella typhimurium using a colorimetric paper-based analytical device coupled with immunomagnetic separation, Anal. Chem. 90 (2018) 1035–1043, https://doi.org/10.1021/acs.analchem.7b04628.
[152] S.U. Son, S.B. Seo, S. Jang, J. Choi, J. woo Lim, D.K. Lee, H. Kim, S. Seo, T. Kang, J. Jung, E.K. Lim, Naked-eye detection of pandemic influenza a (pH1N1) virus by polydiacetylene (PDA)-based paper sensor as a point-of-care diagnostic platform, Sensor. Actuator. B Chem. 291 (2019) 257–265, https://doi.org/10.1016/j.snb.2019.04.081.
[153] H. Wang, L. Yang, S. Chu, B. Liu, Q. Zhang, L. Zou, S. Yu, C. Jiang, Semiquantitative visual detection of lead ions with a smartphone via a colorimetric paper-based analytical device, Anal. Chem. 91 (2019) 9292–9299, https://doi.org/10.1021/acs.analchem.9b02297.
[154] K.N. Han, J.S. Choi, J. Kwon, Gold nanozyme-based paper chip for colorimetric detection of mercury ions, Sci. Rep. 7 (2017), https://doi.org/10.1038/s41598-017-02948-x.
[155] A. Alba-Patiño, S.M. Russell, R. de la Rica, Origami-enabled signal amplification for paper-based colorimetric biosensors, Sensor. Actuator. B Chem. 273 (2018) 951–954, https://doi.org/10.1016/j.snb.2018.07.019.
[156] Y.H. Ngo, D. Li, G.P. Simon, G. Garnier, Gold nanoparticle-paper as a three-dimensional surface enhanced Raman scattering substrate, Langmuir 28 (2012) 8782–8790, https://doi.org/10.1021/la3012734.
[157] M.J. Oliveira, P. Quaresma, M.P. de Almeida, A. Araújo, E. Pereira, E. Fortunato, R. Martins, R. Franco, H. Águas, Office paper decorated with silver nanostars-an alternative cost effective platform for trace analyte detection by SERS, Sci. Rep. 7 (2017), https://doi.org/10.1038/s41598-017-02484-8.
[158] S.S.B. Moram, C. Byram, S.N. Shibu, B.M. Chilukamarri, V.R. Soma, Ag/Au nanoparticle-loaded paper-based versatile surface-enhanced Raman spectroscopy substrates for multiple explosives detection, ACS Omega 3 (2018) 8190–8201, https://doi.org/10.1021/acsomega.8b01318.
[159] S.W. Hu, S. Qiao, J. bin Pan, B. Kang, J.J. Xu, H.Y. Chen, A paper-based SERS test strip for quantitative detection of Mucin-1 in whole blood, Talanta 179 (2018) 9–14, https://doi.org/10.1016/j.talanta.2017.10.038.
[160] M. Lee, K. Oh, H.K. Choi, S.G. Lee, H.J. Youn, H.L. Lee, D.H. Jeong, Subnanomolar sensitivity of filter paper-based SERS sensor for pesticide detection by hydrophobicity change of paper surface, ACS Sens. 3 (2018) 151–159, https://doi.org/10.1021/acssensors.7b00782.
[161] H.T. Chorsi, H.T. Chorsi, J.X.J. Zhang, Using Graphene Plasmonics to Boost Biosensor Sensitivity, SPIE Newsroom, 2016, https://doi.org/10.1117/2.1201610.006712.
[162] N.A.S. Omar, Y.W. Fen, J. Abdullah, A.R. Sadrolhosseini, Y. Mustapha Kamil, N.I.M. Fauzi, H.S. Hashim, M.A. Mahdi, Quantitative and selective surface plasmon resonance response based on a reduced graphene oxide–polyamidoamine nanocomposite for detection of dengue virus E-proteins, Nanomaterials 10 (2020) 569, https://doi.org/10.3390/nano10030569.
[163] M. Srisa-Art, K.E. Boehle, B.J. Geiss, C.S. Henry, Highly sensitive detection of Salmonella typhimurium using a colorimetric paper-based analytical device coupled with immunomagnetic separation, Anal. Chem. 90 (2018) 1035–1043, https://doi.org/10.1021/acs.analchem.7b04628.
[164] S.U. Son, S.B. Seo, S. Jang, J. Choi, J. Lim, D.K. Lee, H. Kim, S. Seo, T. Kang, J. Jung, E.-K. Lim, Naked-eye detection of pandemic influenza a (pH1N1) virus by polydiacetylene (PDA)-based paper sensor as a point-of-care diagnostic platform, Sensor. Actuator. B Chem. 291 (2019) 257–265, https://doi.org/10.1016/j.snb.2019.04.081.
[165] T. Riedel, F. Surman, S. Hageneder, O. Pop-Georgievski, C. Noehammer, M. Hofner, E. Brynda, C. Rodriguez-Emmenegger, J. Dostálek, Hepatitis B plasmonic biosensor for the analysis of clinical serum samples, Biosens. Bioelectron. 85 (2016) 272–279, https://doi.org/10.1016/j.bios.2016.05.014.
[166] S.K. Vashist, E. Marion Schneider, R. Zengerle, F. von Stetten, J.H.T. Luong, Graphene-based rapid and highly-sensitive immunoassay for C-reactive protein using a smartphone-based colorimetric reader, Biosens. Bioelectron. 66 (2015) 169–176, https://doi.org/10.1016/j.bios.2014.11.017.
[167] H.T. Chorsi, Y. Zhu, J.X.J. Zhang, Patterned plasmonic surfaces—theory, fabrication, and applications in biosensing, J. Microelectromech. Syst. 26 (2017) 718–739, https://doi.org/10.1109/JMEMS.2017.2699864.
[168] W. Xu, L. Wang, R. Zhang, X. Sun, L. Huang, H. Su, X. Wei, C.-C. Chen, J. Lou, H. Dai, K. Qian, Diagnosis and prognosis of myocardial infarction on a plasmonic chip, Nat. Commun. 11 (2020) 1654, https://doi.org/10.1038/s41467-020-15487-3.
[169] B.A. Prabowo, Y.-F. Chang, H.-C. Lai, A. Alom, P. Pal, Y.-Y. Lee, N.-F. Chiu, K. Hatanaka, L.-C. Su, K.-C. Liu, Rapid screening of Mycobacterium tuberculosis complex (MTBC) in clinical samples by a modular portable biosensor, Sensor. Actuator. B Chem. 254 (2018) 742–748, https://doi.org/10.1016/j.snb.2017.07.102.

[170] N.A.S. Omar, Y.W. Fen, J. Abdullah, Y. Mustapha Kamil, W.M.E.M.M. Daniyal, A.R. Sadrolhosseini, M.A. Mahdi, Sensitive detection of dengue virus type 2 E-proteins signals using self-assembled monolayers/reduced graphene oxide-PAMAM dendrimer thin film-SPR optical sensor, Sci. Rep. 10 (2020) 2374, https://doi.org/10.1038/s41598-020-59388-3.
[171] B. Zhang, R.B. Kumar, H. Dai, B.J. Feldman, A plasmonic chip for biomarker discovery and diagnosis of type 1 diabetes, Nat. Med. 20 (2014) 948–953, https://doi.org/10.1038/nm.3619.
[172] X. Li, T. Kuznetsova, N. Cauwenberghs, M. Wheeler, H. Maecker, J.C. Wu, F. Haddad, H. Dai, Autoantibody profiling on a plasmonic nano-gold chip for the early detection of hypertensive heart disease, Proc. Natl. Acad. Sci. Unit. States Am. 114 (2017) 7089–7094, https://doi.org/10.1073/pnas.1621457114.
[173] P.P. Austin Suthanthiraraj, A.K. Sen, Localized surface plasmon resonance (LSPR) biosensor based on thermally annealed silver nanostructures with on-chip blood-plasma separation for the detection of dengue non-structural protein NS1 antigen, Biosens. Bioelectron. 132 (2019) 38–46, https://doi.org/10.1016/j.bios.2019.02.036.
[174] J. Zhou, F. Tao, J. Zhu, S. Lin, Z. Wang, X. Wang, J.-Y. Ou, Y. Li, Q.H. Liu, Portable tumor biosensing of serum by plasmonic biochips in combination with nanoimprint and microfluidics, Nanophotonics 8 (2019) 307–316, https://doi.org/10.1515/nanoph-2018-0173.
[175] Z. Geng, Q. Kan, J. Yuan, H. Chen, A route to low-cost nanoplasmonic biosensor integrated with optofluidic-portable platform, Sensor. Actuator. B Chem. 195 (2014) 682–691, https://doi.org/10.1016/j.snb.2014.01.110.
[176] N.L. Garrett, R. Sekine, M.W.A. Dixon, L. Tilley, K.R. Bambery, B.R. Wood, Bio-sensing with butterfly wings: naturally occurring nano-structures for SERS-based malaria parasite detection, Phys. Chem. Chem. Phys. 17 (2014) 21164–21168, https://doi.org/10.1039/c4cp04930f.
[177] W. Diao, M. Tang, S. Ding, X. Li, W. Cheng, F. Mo, X. Yan, H. Ma, Y. Yan, Highly sensitive surface plasmon resonance biosensor for the detection of HIV-related DNA based on dynamic and structural DNA nanodevices, Biosens. Bioelectron. 100 (2018) 228–234, https://doi.org/10.1016/j.bios.2017.08.042.
[178] M. Trzaskowski, A. Napiórkowska, E. Augustynowicz-Kopeć, T. Ciach, Detection of tuberculosis in patients with the use of portable SPR device, Sensor. Actuator. B Chem. 260 (2018) 786–792, https://doi.org/10.1016/j.snb.2017.12.183.
[179] P.K. Sharma, J.S. Kumar, V.v. Singh, U. Biswas, S.S. Sarkar, S.I. Alam, P.K. Dash, M. Boopathi, K. Ganesan, R. Jain, Surface plasmon resonance sensing of Ebola virus: a biological threat, Anal. Bioanal. Chem. 412 (2020) 4101–4112, https://doi.org/10.1007/s00216-020-02641-5.
[180] H. Wan, C. Merriman, M.A. Atkinson, C.H. Wasserfall, K.M. Mcgrail, Y. Liang, D. Fu, H. Dai, Proteoliposome-based full-length ZnT8 self-antigen for type 1 diabetes diagnosis on a plasmonic platform, Proc. Natl. Acad. Sci. Unit. States Am. 114 (2017) 10196–10201, https://doi.org/10.1073/pnas.1711169114.
[181] A. Belushkin, F. Yesilkoy, J.J. González-López, J.C. Ruiz-Rodríguez, R. Ferrer, A. Fàbrega, H. Altug, Rapid and digital detection of inflammatory biomarkers enabled by a novel portable nanoplasmonic imager, Small 16 (2020) 1906108, https://doi.org/10.1002/smll.201906108.
[182] T.J. Palinski, A. Tadimety, I. Trase, B.E. Vyhnalek, G.W. Hunter, E. Garmire, J.X.J. Zhang, Vibrant reflective sensors with percolation film Fabry-Pérot nanocavities, Opt Express 29 (2021) 25000, https://doi.org/10.1364/oe.432097.
[183] K. Leosson, A.S. Ingason, B. Agnarsson, A. Kossoy, S. Olafsson, M.C. Gather, Ultra-thin gold films on transparent polymers, Nanophotonics 2 (2013) 3–11, https://doi.org/10.1515/nanoph-2012-0030.
[184] V. Krachmalnicoff, E. Castanié, Y. de Wilde, R. Carminati, Fluctuations of the Local Density of States Probe Localized Surface Plasmons on Disordered Metal Films, 2010, pp. 183901–183902, https://doi.org/10.1103/PhysRevLett.105.183901.
[185] R. Malureanu, A. Lavrinenko, Ultra-thin films for plasmonics: a technology overview, Nanotechnol. Rev. 4 (2015) 259–275, https://doi.org/10.1515/ntrev-2015-0021.
[186] M. Kang, S.G. Park, K.H. Jeong, Repeated solid-state dewetting of thin gold films for nanogap-rich plasmonic nanoislands, Sci. Rep. 5 (2015) 1–7, https://doi.org/10.1038/srep14790.
[187] S.M. Tabakman, Z. Chen, H.S. Casalongue, H. Wang, H. Dai, A new approach to solution-phase gold seeding for SERS substrates, Small 7 (2011) 499–505, https://doi.org/10.1002/smll.201001836.
[188] M. Kang, S.G. Park, K.H. Jeong, Repeated solid-state dewetting of thin gold films for nanogap-rich plasmonic nanoislands, Sci. Rep. 5 (2015) 1–7, https://doi.org/10.1038/srep14790.
[189] X. Sun, H. Li, Gold nanoisland arrays by repeated deposition and post-deposition annealing for surface-enhanced Raman spectroscopy, Nanotechnology 24 (2013) 355706, https://doi.org/10.1088/0957-4484/24/35/355706.
[190] A. Bonyár, I. Csarnovics, M. Veres, L. Himics, A. Csik, J. Kámán, L. Balázs, S. Kökényesi, Investigation of the performance of thermally generated gold nanoislands for LSPR and SERS applications, Sensor. Actuator. B Chem. 255 (2018) 433–439, https://doi.org/10.1016/J.SNB.2017.08.063.
[191] B. Miranda, K.-Y. Chu, P.L. Maffettone, A.Q. Shen, R. Funari, Metal-enhanced fluorescence immunosensor based on plasmonic arrays of gold nanoislands on an etched glass substrate, ACS Appl. Nano Mater. 3 (2020) 10470–10478, https://doi.org/10.1021/acsanm.0c02388.
[192] D. Wang, R. Ji, P. Schaaf, Formation of precise 2D Au particle arrays via thermally induced dewetting on pre-patterned substrates, Beilstein J. Nanotechnol. 2 (2011) 318–326, https://doi.org/10.3762/bjnano.2.37.
[193] H.T.H. Lin, C.K. Yang, C.C. Lin, A.M.H. Wu, L.A. Wang, N.T. Huang, A large-area nanoplasmonic sensor fabricated by rapid thermal annealing treatment for label-free and multi-point immunoglobulin sensing, Nanomaterials 7 (2017), https://doi.org/10.3390/nano7050100.
[194] W. Xu, L. Wang, R. Zhang, X. Sun, L. Huang, H. Su, X. Wei, C.C. Chen, J. Lou, H. Dai, K. Qian, Diagnosis and prognosis of myocardial infarction on a plasmonic chip, Nat. Commun. 11 (2020) 1654, https://doi.org/10.1038/s41467-020-15487-3.
[195] R. Zhang, B. Le, W. Xu, K. Guo, X. Sun, H. Su, L. Huang, J. Huang, T. Shen, T. Liao, Y. Liang, J.X.J. Zhang, H. Dai, K. Qian, Magnetic "squashing" of circulating tumor cells on plasmonic substrates for ultrasensitive NIR fluorescence detection, Small Methods 3 (2019) 1800474, https://doi.org/10.1002/smtd.201800474.
[196] S.M. Tabakman, L. Lau, J.T. Robinson, J. Price, S.P. Sherlock, H. Wang, B. Zhang, Z. Chen, S. Tangsombatvisit, J.A. Jarrell, P.J. Utz, H. Dai, Plasmonic substrates for multiplexed protein microarrays with femtomolar sensitivity and broad dynamic range, Nat. Commun. 2 (2011) 466, https://doi.org/10.1038/ncomms1477.
[197] B. Liu, Y. Li, H. Wan, L. Wang, W. Xu, S. Zhu, Y. Liang, B. Zhang, J. Lou, H. Dai, K. Qian, High performance, multiplexed lung cancer biomarker detection on a plasmonic gold chip, Adv. Funct. Mater. 26 (2016) 7994–8002, https://doi.org/10.1002/adfm.201603547.
[198] J.R. Choi, Development of point-of-care biosensors for COVID-19, Front. Chem. 8 (2020), https://doi.org/10.3389/fchem.2020.00517.
[199] A. Parihar, P. Ranjan, S.K. Sanghi, A.K. Srivastava, R. Khan, Point-of-Care biosensor-based diagnosis of COVID-19 holds promise to combat current and future pandemics, ACS Appl. Bio Mater. 3 (2020) 7326–7343, https://doi.org/10.1021/acsabm.0c01083.
[200] Y. Rasmi, X. Li, J. Khan, T. Ozer, J.R. Choi, Emerging point-of-care biosensors for rapid diagnosis of COVID-19: current progress, challenges, and future prospects, Anal. Bioanal. Chem. 413 (2021) 4137–4159, https://doi.org/10.1007/s00216-021-03377-6.
[201] A.M. Shrivastav, U. Cvelbar, I. Abdulhalim, A comprehensive review on plasmonic-based biosensors used in viral diagnostics, Commun. Biol. 4 (2021) 1–12, https://doi.org/10.1038/s42003-020-01615-8.
[202] A. Djaileb, B. Charron, M.H. Jodaylami, V. Thibault, J. Coutu, K. Stevenson, S. Forest, L.S. Live, D. Boudreau, J.N. Pelletier, J.F. Masson, A rapid and quantitative serum test for SARS-CoV-2 antibodies with portable surface plasmon resonance sensing, ChemRxiv (2020) 1–12, https://doi.org/10.26434/chemrxiv.12118914.
[203] G. Qiu, Z. Gai, Y. Tao, J. Schmitt, G.A. Kullak-Ublick, J. Wang, Dual-functional plasmonic photothermal biosensors for highly accurate severe acute respiratory syndrome coronavirus 2 detection, ACS Nano 14 (2020) 5268–5277, https://doi.org/10.1021/acsnano.0c02439.
[204] A.N. Masterson, B.B. Muhoberac, A. Gopinadhan, D.J. Wilde, F.T. Deiss, C.C. John, R. Sardar, Multiplexed and high-throughput label-free detection of RNA/spike protein/IgG/IgM biomarkers of SARS-CoV-2 infection utilizing nanoplasmonic biosensors, Anal. Chem. 93 (2021) 8754–8763, https://doi.org/10.1021/acs.analchem.0c05300.
[205] X. Peng, Y. Zhou, K. Nie, F. Zhou, Y. Yuan, J. Song, J. Qu, Promising near-infrared plasmonic biosensor employed for specific detection of SARS-CoV-2 and its spike glycoprotein, New J. Phys. 22 (2020), https://doi.org/10.1088/1367-2630/abbe53.
[206] D. Li, H. Zhou, X. Hui, X. He, X. Mu, Plasmonic biosensor augmented by a genetic algorithm for ultra-rapid, label-free, and multi-functional detection of COVID-19, Anal. Chem. 93 (2021) 9437–9444, https://doi.org/10.1021/acs.analchem.1c01078.
[207] P. Moitra, M. Alafeef, M. Alafeef, M. Alafeef, K. Dighe, M.B. Frieman, D. Pan, D. Pan, D. Pan, Selective naked-eye detection of SARS-CoV-2 mediated by N gene targeted antisense oligonucleotide capped plasmonic nanoparticles, ACS Nano 14 (2020) 7617–7627, https://doi.org/10.1021/acsnano.0c03822.
[208] X. Li, J. Shu, W. Gu, L. Gao, Deep neural network for plasmonic sensor modeling, Opt. Mater. Express 9 (2019) 3857, https://doi.org/10.1364/ome.9.003857.
[209] Z.S. Ballard, D. Shir, A. Bhardwaj, S. Bazargan, S. Sathianathan, A. Ozcan, Computational sensing using low-cost and mobile plasmonic readers designed by machine learning, ACS Nano 11 (2017) 2266–2274, https://doi.org/10.1021/acsnano.7b00105.
[210] G. Moon, J. ryul Choi, C. Lee, Y. Oh, K.H. Kim, D. Kim, Machine learning-based design of meta-plasmonic biosensors with negative index metamaterials, Biosens. Bioelectron. 164 (2020), https://doi.org/10.1016/j.bios.2020.112335.
[211] J. He, C. He, C. Zheng, Q. Wang, J. Ye, Plasmonic nanoparticle simulations and inverse design using machine learning, Nanoscale 11 (2019) 17444–17459, https://doi.org/10.1039/c9nr03450a.
[212] I. Malkiel, M. Mrejen, A. Nagler, U. Arieli, L. Wolf, H. Suchowski, Plasmonic nanostructure design and characterization via Deep Learning, Light Sci. Appl. 7 (2018), https://doi.org/10.1038/s41377-018-0060-7.
[213] Institute of Electrical and Electronics Engineers, in: 13th International Conference on Software, Knowledge, Information Management and Applications (SKIMA), 2019 (n.d).
[214] M.K. Song, S.X. Chen, P.P. Hu, C.Z. Huang, J. Zhou, Automated plasmonic resonance scattering imaging analysis via deep learning, Anal. Chem. 93 (2021) 2619–2626, https://doi.org/10.1021/acs.analchem.0c04763.
[215] M. Erzina, A. Trelin, O. Guselnikova, B. Dvorankova, K. Strnadova, A. Perminova, P. Ulbrich, D. Mares, V. Jerabek, R. Elashnikov, V. Svorcik, O. Lyutakov, Precise cancer detection via the combination of functionalized SERS surfaces and convolutional neural network with independent inputs, Sensor. Actuator. B Chem. 308 (2020), https://doi.org/10.1016/j.snb.2020.127660.
[216] K.M. Hanafiah, M. Garcia, D. Anderson, Point-of-care testing and the control of infectious diseases, Biomarkers Med. 7 (2013) 333–347, https://doi.org/10.2217/bmm.13.57.

[217] C. Tymm, J. Zhou, A. Tadimety, A. Burklund, J.X.J. Zhang, Scalable COVID-19 detection enabled by lab-on-chip biosensors, Cell. Mol. Bioeng. 13 (2020) 313–329, https://doi.org/10.1007/s12195-020-00642-z.

[218] R. Lei, R. Huo, C. Mohan, Current and emerging trends in point-of-care urinalysis tests, Expert Rev. Mol. Diagn. 20 (2020) 69–84, https://doi.org/10.1080/14737159.2020.1699063.

[219] M.N. Esbin, O.N. Whitney, S. Chong, A. Maurer, X. Darzacq, R. Tjian, Overcoming the bottleneck to widespread testing: a rapid review of nucleic acid testing approaches for COVID-19 detection, RNA 26 (2020) 771–783, https://doi.org/10.1261/rna.076232.120.

[220] P. Rai, B.K. Kumar, V.K. Deekshit, I. Karunasagar, I. Karunasagar, Detection technologies and recent developments in the diagnosis of COVID-19 infection, Appl. Microbiol. Biotechnol. 105 (2021) 441–455, https://doi.org/10.1007/s00253-020-11061-5.

[221] L. Dong, C. Jin, A.B. Closson, I. Trase, H.R. Richards, Z. Chen, J.X.J. Zhang, Cardiac energy harvesting and sensing based on piezoelectric and triboelectric designs, Nano Energy 76 (2020) 105076, https://doi.org/10.1016/j.nanoen.2020.105076.

[222] C. Jin, N. Hao, Z. Xu, I. Trase, Y. Nie, L. Dong, A. Closson, Z. Chen, J.X.J. Zhang, Flexible piezoelectric nanogenerators using metal-doped ZnO-PVDF films, Sens. Actuators, A 305 (2020) 111912, https://doi.org/10.1016/j.sna.2020.111912.

[223] Z. Xu, C. Jin, A. Cabe, D. Escobedo, N. Hao, I. Trase, A.B. Closson, L. Dong, Y. Nie, J. Elliott, M.D. Feldman, Z. Chen, J.X.J. Zhang, Flexible energy harvester on a pacemaker lead using multibeam piezoelectric composite thin films, ACS Appl. Mater. Interfaces 12 (2020) 34170–34179, https://doi.org/10.1021/acsami.0c07969.

[224] L. Dong, A.B. Closson, C. Jin, Y. Nie, A. Cabe, D. Escobedo, S. Huang, I. Trase, Z. Xu, Z. Chen, M.D. Feldman, J.X.J. Zhang, Multifunctional pacemaker lead for cardiac energy harvesting and pressure sensing, Adv. Healthc. Mater. 9 (2020), https://doi.org/10.1002/adhm.202000053.

[225] C. Jin, L. Dong, Z. Xu, A. Closson, A. Cabe, A. Gruslova, S. Jenney, D. Escobedo, J. Elliott, M. Zhang, N. Hao, Z. Chen, M.D. Feldman, J.X.J. Zhang, Skin-like elastomer embedded zinc oxide nanoarrays for biomechanical energy harvesting, Adv. Mater. Interfac. (2021) 1–10, https://doi.org/10.1002/admi.202100094, 2100094.

[226] Z. Xu, C. Jin, A. Cabe, D. Escobedo, A. Gruslova, S. Jenney, A.B. Closson, L. Dong, Z. Chen, M.D. Feldman, J.X.J. Zhang, Implantable cardiac kirigami-inspired lead-based energy harvester fabricated by enhanced piezoelectric composite film, Adv. Healthc. Mater. 10 (2021) 1–9, https://doi.org/10.1002/adhm.202002100.